Parking search in the physical world: Calculating the search time by leveraging physical and graph theoretical methods

Nilankur Dutta, Thibault Charlottin, Alexandre Nicolas

Parking search in the physical world: Calculating the search time by leveraging physical and graph theoretical methods

Nilankur DUTTA
Institut Lumière Matière, CNRS and Université Claude Bernard Lyon 1,
F-69622 Villeurbanne, France, nilankur.dutta@gmail.com

Thibault CHARLOTTIN
Institut Lumière Matière, CNRS and Université Claude Bernard Lyon 1,
F-69622 Villeurbanne, France, and
École nationale des travaux publics de l'État (ENTPE), Université de Lyon,
F-69518 Vaulx-en-Velin, France

Alexandre NICOLAS
Institut Lumière Matière, CNRS and Université Claude Bernard Lyon 1,
F-69622 Villeurbanne, France, alexandre.nicolas@polytechnique.edu, https://www.alexandrenicolas.net

Parking plays a central role in transport policies and has wide-ranging consequences: While the average time spent searching for parking exceeds dozens of hours per driver every year in many Western cities, the associated cruising traffic generates major externalities, by emitting pollutants and contributing to congestion. However, the laws governing the parking search time remain opaque in many regards, which hinders any general understanding of the problem and its determinants. Here, we frame the problem of parking search in a very generic, but mathematically compact formulation which puts the focus on the role of the street network and the unequal attractiveness of parking spaces. This problem is solved in two independent ways, valid in any street network and for a wide range of drivers' behaviours. Numerically, this is done by means of a computationally efficient and versatile agent-based model. Analytically, we leverage the machinery of Statistical Physics and Graph Theory to derive a generic mean-field relation giving the parking search time as a function of the occupancy of parking spaces; an expression for the latter is obtained in the stationary regime. We show that these theoretical results are applicable in toy networks as well as in complex, realistic cases such as the large-scale street network of the city of Lyon, France. Taken as a whole, these findings clarify the parameters that directly control the search time and provide transport engineers with a quantitative grasp of the parking problem. Besides, they establish formal connections between the parking issue in realistic settings and physical problems.

Key words: on-street parking; parking search time; street network; graph theory

1. Introduction

Cars are designed to move, but paradoxically whether or not to use this mode of transportation is oftentimes less a matter of *driving to* a certain destination than being able to *park*

there. Indeed, in many large metropolitan areas, it is hard to overstate the importance of parking on mobility choices and, more broadly, daily life in a city (Shoup 2018): The time spent searching for parking exceeds dozens of hours per driver every year (35h to 107h in Western metropolises, according to INRIX survey data (Cookson and Pishue 2017)), at an estimated cost of several hundred Euros a year per driver. The burden of parking search is nonetheless unequally shared among drivers and trips: the many trips ended without any cruising contrast with the very long search times experienced in some cases (Mantouka, Fafoutellis, and Vlahogianni 2021). Furthermore, trips that motorists eventually give up because of the lack of parking space are not uncommon. (For example, a 2005 survey conducted in 3 French cities indicated that the percentage of interviewees who had at least once given up a trip ('balking') because of parking unavailability amounted to 48% in Grenoble, 67% in Lyon, and 100% in Paris (SARECO / Prédit-Ademe 2005).) Beyond these individual quandaries, cars cruising for parking may represent more than 10% of the total traffic in many large cities (e.g., 15% in central Stuttgart, 28% to 45% in New York), according to surveys and observations of the number of cars driving by a vacant spot before it is occupied (Shoup 2018, Hampshire and Shoup 2018); these cruising cars contribute to congestion and pollution in city centres (Gallo, D'Acierno, and Montella 2011). Admittedly, these quantitative figures are vividly debated and may overestimate the typical share of traffic due to cruising for parking by investigating only the most problematic areas (Weinberger, Millard-Ball, and Hampshire 2020).

Still, there is a broad consensus about the centrality of parking in transport policies. While some cities require developers to add a parking facility to their development plans, through so called minimum parking requirements (Shoup 2018, chap. 3), in many others restrictive parking policies have become an essential lever of action for transport authorities (Boujnah 2017, Polak and Axhausen 1990) to curb down the use of private cars, notably as a response to climate change. Besides, smart cities are on the rise and intend to alleviate the pains of parking thanks to dynamic parking information and the possibility to book a parking spot, as well as parking guidance systems (Al-Turjman and Malekloo 2019).

These points call for more reliable observations of the current state of parking in different contexts, but also for a deeper understanding of the process of parking search, so as to be able to predict the impact of hypothetical measures. However, for all its importance, the topic of parking is still fairly opaque, with a limited intuitive grasp of its main factors and their quantitative impact. This dim understanding is not surprising given the complexity of the problem, which mingles socio-psychological and economic factors with physical constraints and collective effects. Some seemingly natural assumptions about the relation between occupancy and parking search time (Axhausen et al. 1994, Arnott and Williams 2017) are commonly used (Geroliminis 2015), but can hardly be reconciled with facts (see Sec. 2.2).

In this paper, the problem of searching for parking is framed in a way that is both defined in a mathematically concise way and more versatile than existing agent-based approaches, so as to gain quantitative insight into the parking search process in general. The focus is put on the role of the street network and the unequal attractiveness of parking spaces (due to their location and rates, for instance) among other blind spots of existing approaches (Section 2); some more studied effects, notably the medium-term elasticity of parking demand (briefly touched on in the conclusion), are brushed aside. Interesting parallels with problems in the realm of Physics (Schadschneider, Chowdhury, and Nishinari 2010), more precisely the asymmetric motion of active particles on a graph, then become apparent and clarify some facets of parking search. Importantly, once thus formulated, the parking search problem can be solved not only by means of a computationally efficient agent-based algorithm that we developed, but also by leveraging the powerful machinery of Statistical Physics and Graph Theory (Section 3). This leads to analytical formulae for the search time and for the steady-state occupancy. These hold in remarkably generic settings, for any street network and for a

wide range of driving strategies and parking choices, provided that circling is not too intensive. These theoretical results are found to be applicable in toy networks as well as in the complex, large-scale case of the city of Lyon, France (Section 4). For sure, some input parameters of the model, first of which the drivers' route choices and their perceptions of the attractiveness of parking spots, must be adjusted depending on the context. However, irrespective of these adjustments, our methods are instrumental in advancing the quantitative understanding of parking search determinants beyond case-by-case (city-specific) findings. They also pave the way for theoretical assessments of e.g. the excess emissions of pollutants due to cruising for parking or the efficiency of smart parking solutions.

2. Blind Spots of existing Approaches to Parking Search

2.1. Literature survey of the determinants of the parking search behaviour

The behaviours and strategies of drivers in search of parking have been probed by means of field observations ('revealed preferences'), surveys ('stated preferences'), and more recently virtual experiments (Fulman, Benenson, and Elia 2020). Among the factors that influence parking behaviour, pricing has been intensely studied and plays a major role in parking choice (Brooke, Ison, and Quddus 2014, Shoup 2018, Gao et al. 2021), which has prompted dynamic pricing strategies to control the occupancy (Chatman and Manville 2014). The price elasticity of parking volume (i.e., the number of cars that parked in a given duration) generally lies in the range $[-2, -0.2]$, but strongly depends on the context, in particular the average occupancy and the existence of substitutes in terms of parking facilities or mode of transportation (transit service); it is also found to be sensitive to the methodology used, with disagreements between stated and revealed preferences (see (Lehner and Peer 2019) for a recent meta-analysis). Of course, the relative prices of alternative parking modes, such as car parks, also affect the drivers' decision to search and possibly cruise for on-street parking or not (Assemi, Baker, and Paz 2020). But, importantly, drivers are not always aware of the real parking price and may have a distorted view of the relative on-street and off-street parking rates (Lee, Agdas, and Baker 2017). Another key determinant of parking choice is the location of the parking space, most prominently the distance to destination both for parking on the curb and for off-street parking. There is a marked preference for spots near the ticket machine (if there is one) in parking lots (Vo, van der Waerden, and Wets 2016) or near the facility of interest in rest areas on expressways (Tanaka, Ohno, and Nakamura 2017) or open parking lots (Paidi et al. 2022). The premium for on-street parking in terms of accessibility and convenience may partly explain the intensity of cruising (Lee, Agdas, and Baker 2017). Other *intrinsic* features of the parking supply contribute to parking choices: the size of the parking space, the availability of boards with parking guidance information, which may have an influence or not depending on the conditions (Axhausen et al. 1994, Tanaka, Ohno, and Nakamura 2017), etc. All these factors (which are to be subsumed into an 'attractiveness' variable in the following) thus influence the parking search process.

But the drivers' experience during parking search, in turn, can also affect their parking decision. Drivers generally abhor long travel times, especially in congested conditions (Gao et al. 2021), and queues (Tanaka, Ohno, and Nakamura 2017). On the basis of surveys conducted in Brisbane, Australia, Assemi, Baker, and Paz (2020) found that the purpose of the trip, the arrival time, the parking frequency, and the on-street parking accumulation all affect cruising for parking. Using GPS tracks collected in the region of Athens, Greece, and exploring the dependencies of the search times with various machine-learning approaches, Mantouka, Fafoutellis, and Vlahogianni (2021) ascertained that arriving in the morning peak hours and/or making longer trips is positively correlated with cruising. Regarding the search

pattern, the typical driver first drives to the vicinity of the destination (85% of times for the participants involved in the parking 'game' set by (Fulman, Benenson, and Elia 2020), where the average on-street occupancy was set to $\phi = 99.7\%$). Then, they start circling around it and possibly spiral farther and farther away from it, before eventually quitting the search or heading for an off-street parking lot, after a few minutes (Fulman, Benenson, and Elia 2020) or more (SARECO / Prédit-Ademe 2005, Levy, Martens, and Benenson 2013, Weinberger, Millard-Ball, and Hampshire 2020, Fulman and Benenson 2021, CEREMA 2015). For drivers that keep searching, the time to park is believed to also depend on the turnover rate of parked vehicles (SARECO / Prédit-Ademe 2005) and the competition with other cruising cars (SARECO / Prédit-Ademe 2005, Arnott and Williams 2017). We will nuance this belief below.

2.2. Real search times elude common approaches

Despite the interdependence of the search time T_s and parking choices, it is tempting to try and assess the former on the basis of simple considerations. To this end, and throughout the paper, let us consider a situation in which we know the parking supply and the global volume of parking demand (they are thus held constant). Supposing that the average occupancy ϕ of parking spots can be measured, a basic but nonetheless very common approximation (Anderson and De Palma 2004, Geroliminis 2015) assumes that cars move along lanes of spots that are randomly occupied with uniform probability ϕ, and park in the first available space that they encounter. This is the theoretical foundation of the *binomial approximation*

$$T_s \simeq \frac{T_0}{1-\phi},$$

where T_0 is the time to drive from one spot to the next one. According to this formula, for $\phi \leqslant 99\%$, the mean search time cannot be significantly longer than $100\,T_0$, which is around one minute if spots are adjacent. This result is manifestly at odds with the empirical observation of surging search times long before ϕ reaches 100% (Arnott and Williams 2017, Gu et al. 2020, Weinberger, Millard-Ball, and Hampshire 2020); in San Francisco, Weinberger, Millard-Ball, and Hampshire (2020) even suggest the blocks where cruising cars eventually park might be occupied only at $\phi = 59\%$. In any event, the time to park is drastically underestimated by this approximation and *ad hoc* corrections to mitigate the discrepancy issue (Belloche 2015) are devoid of theoretical ground. Leclercq, Sénécat, and Mariotte (2017) proposed a theoretically better grounded extension of the binomial approximation, by positing that drivers cover a distance l_{ns} without no parking spaces, before finding m successive spots. The resulting equation provides better fits to the empirical data, at the expense of two additional parameters which need to be calibrated individually for each area under study and are found to vary widely. For their part, Arnott and Williams (2017) rationalised the underestimation of parking search times by the following factors:

1. there are spatial correlations between occupied spots (this 'bunching' effect was later addressed analytically by Krapivsky and Redner (2019, 2020) and by Dowling, Ratliff, and Zhang (2019) in their non-uniform queuing networks; an approximate expression was proposed by Fulman and Benenson (2021) if the per-block occupancy is known),
2. the occupancy is not constant in time, but undergoes statistical fluctuations, and periods of higher occupancy have a stronger impact on the mean search time,
3. the competition between searching cars aggravates the difficulty of the search,
4. circling leads to inefficient double checks.

A simple model with cars moving along a circle strewn with 100 spots and parking in the first available spot was simulated to illustrate these effects. It yielded search times 44% larger than the binomial estimate at an occupancy $\phi \leqslant 67\%$; unfortunately, the authors could not explain this effect from an analytical standpoint. An identical circular geometry and indiscriminate 'park-if-vacant' rule had been used in the probabilistic framework developed by Cao and Menendez (2015). More broadly speaking, it is critical to realise that the parking occupancy ϕ is a spatio-temporal aggregate, obtained by averaging observations over a geographic area and sampling them in, or averaging them over, a time period. (Incidentally, more sophisticated methods have emerged to afford access to the occupancy at higher resolution (Yang and Qian 2017)). Since the relation between occupancy and search time is non-linear, this averaging procedure washes away the oversized impact of long cruising times near hot spots at rush hours.

On the other hand, Weinberger, Millard-Ball, and Hampshire (2020) insist on the role of the drivers' idiosyncratic behaviours in generating excess travel distances (perhaps they have kept driving because they were arguing about where to go for dinner or trying to lull a baby to sleep); the excess travel may be misconstrued as cruising (e.g., using GPS data) in districts of San Francisco and Ann Arbor where there is actually no lack of vacant spots. For the specific case of San Francisco, Millard-Ball, Hampshire, and Weinberger (2020) further note that (even in districts with high parking tension) cruising may actually be rare because the scarcity of vacant spots may be internalised in the regular drivers' behaviours and 'perceived parking scarcity leads drivers to stop short of their destinations', thus curtailing cruising. However, these caveats do not suppress the ample evidence of cruising for parking in other cities (SARECO / Prédit-Ademe 2005, Shoup 2006, Hampshire and Shoup 2018, Cookson and Pishue 2017) as well as off-street parking lots (Paidi et al. 2022).

To settle the debate about the actual parking pain, it is essential to gain insight into what governs the parking search time and its dependence on the occupancy in realistic settings. The following sections will blaze a theoretical trail to do so in a rigorous and generic way. But let us first highlight the influence on parking search of oft-overlooked features, in particular the topology of the explored street network and the fact that parking spaces are not equally attractive to drivers. These effects will be illustrated with particularly simple, somewhat caricatural examples in this section, before delving into the technical complexity of more realistic settings.

2.3. Topology of the street network

While previous *theoretical* endeavours have generally considered linear or circular geometries for parking lanes (Levy, Martens, and Benenson 2013, Cao and Menendez 2015, Krapivsky and Redner 2019, 2020, Arnott and Williams 2017), in reality parking spaces are located on a geometrically more complex network of streets (or alleys in the case of a parking lot), whose topology constrains the motion of the cars. Specific street networks have been studied *numerically*, with a more or less realistic description of their characteristics (see the review in (Boujnah 2017)); to single out only one example, Gallo, D'Acierno, and Montella (2011) simulated the road network of the city of Benevento, Italy, using a a multi-layer model that decouples the in-vehicle trip to the destination (with its specific cost for traffic assignment) from the following cruising part. Dowling, Ratliff, and Zhang (2019) made theoretical progress in the study of street networks with nodes of non-uniform degrees. But the sensitivity of parking search times to the topology has not been investigated.

Nevertheless, it is easy to understand that, for an equal number of on-street spots, their spatial distribution and the topology of the street network will affect the disutility associated

with parking. First consider the simple case illustrated in Fig. 1a with a single major destination point (hot spot) and no off-street parking facility. Under equal demand, parking issues will be all the more severe as they are few streets allowing parking on the curb that lead to the hot spot. With fewer incoming streets, it will be harder to find a spot close enough to the destination.

Even if drivers park in the first vacant spot that they encounter, the network topology will matter. To understand this, we turn to the two examples of parking lots displayed in Fig. 1b, where cars are injected at constant rate at the entrance and spots are located at exactly the same positions in space but are not accessible in the same way: In topology (A), cars enter one of the 9 parallel rows from the main alley at the top of the sketch, with equal probabilities for each (which is done by setting the turning rates adequately), whereas in topology (B) cars visit the rows sequentially, driving by every spot before returning to the entrance point. At low occupancy, the search time will be mostly constant constant in topology (A), resulting from the travel time along the main alley, whereas it will increase almost linearly with the occupancy in topology (B), as the first spots get more and more occupied. These intuitions are confirmed by the numerical results shown in Fig. 1c (with the protocol detailed in Section 3.2); around $\phi \equiv \phi_c \approx 40\%$, there is a crossover from a low-occupancy situation with shorter searches in topology (B) to the opposite case when $\phi > \phi_c$. At high occupancies ($\phi >$80% or 90%), the mean search time starts to be dominated by the periods of time when the parking lot is full, because of statistical fluctuations, and cars have to circle several times before a parked car leaves. The search time then surges dramatically and diverges to ∞ as $\phi \to 100\%$, with a possibly steeper increase in topology (A), where the rare vacant spot may be found only after several loops (incidentally, this feature will actually elude the mean-field approach proposed below). Obviously, the binomial approximation can explain neither the steepness of this divergence, nor the differences between topologies (A) and (B) at moderate occupancies.

Undoubtedly, these topological effects can hardly be captured by approaches oblivious of the street network. These considerations are not merely abstract: they have contributed to shaping cities and land (Shoup 2018, intro.). This is perhaps best exemplified by the strip geometry of strip malls in North America or retail parks in Europe, which enables customers to park directly in front of the shops.

2.4. Attractiveness of parking spaces

Beyond the (fixed) structure of the street network, the way in which motorists navigate through it also matters. Variations in the cruising strategies have been observed in parking lots by Paidi et al. (2022), but an even more striking example is the anonymous driver observed by Hampshire et al. (2016) who routinely circles around the free parking spaces on the edge of downtown before driving to the paying spaces downtown. Somewhat similarly, some drivers may tend to circle through the very same blocks over and over again, waiting for a spot to be freed, rather than extending their search to neighbouring streets; the recurring driving through the same blocks naturally prolongs the search, compared to the exploration of new blocks. In the same vein, the driver may refrain from parking at the first vacant spot that they encounter and exhibit distinct preferences, for instance balking at parking too far from the destination or in a paying space when there remains a possibility to park for free (Weinberger, Millard-Ball, and Hampshire 2020).

Quantitatively, we choose to gauge the driver's willingness to park at a given spot i by the probability p_i that she will park there *if* she drives by this spot while it is vacant. The distribution of p_i in a neighbourhood clearly affects parking search. For instance, consider the

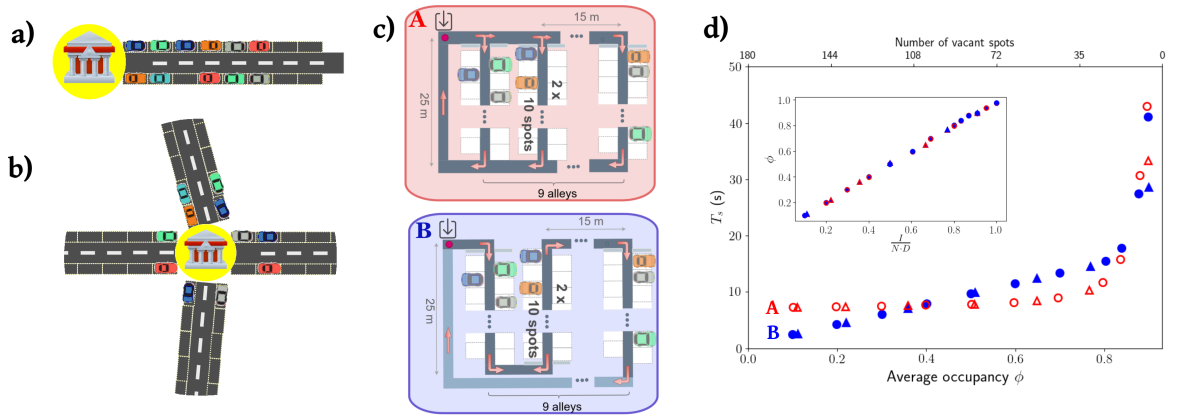

Figure 1 **Influence of the topology of the street network on (a,b) curbside and (c,d) off-street parking. A major destination (hot spot) is located at the extremity of a dead-end street in sketch (a) and at an intersection in sketch (b). Panel (c) displays two model off-street parking lots of $N = 180$ spaces; the evolution of the search time T_s in each, for drivers parking in the first vacant spot, is shown in panel (d) as a function of the average occupancy ϕ. Inset: Relation between ϕ and the product of the injection rate I with the parking time D^{-1} [$D^{-1} = 30\,\mathrm{min}$ for the triangles (△), $60\,\mathrm{min}$ for the circles (◯)].**

'toy' network corresponding to a small neighbourhood of Lyon shown in Fig. 2(a); for the same demand, search times will drastically differ between a situation with equally attractive spaces ($p_i = 100\%$ for every spot i) and a situation in which drivers exhibit a marked preference for two lanes of attractive (e.g., free) spots at $p_i = 100\%$ and balk at parking in other (costly) spots, where $p_i = 1\%$. In the latter case, drivers are prone to circling before finding a vacant free spot and search times sky-rocket even though the network-averaged occupancy remains moderate (as also supported by the numerical simulations displayed in Fig. 2(c)).

This simple example shows how using spatially averaged occupancies to estimate parking difficulties goes completely amiss whenever there is a contrast in spot attractiveness: the high occupancy of attractive spots may be balanced by their vacant counterparts. Fulman and Benenson (2021) recently improved the binomial approximation by taking into account the occupancies averaged over small neighbourhoods instead of the global one and demonstrated that it much better reproduces search times in the presence of bunching (an inherent consequence of the sequential parking process) and a spatially heterogeneous demand. Nevertheless, their approach requires simulations to estimate of the distribution of local occupancies and does not explicitly handle heterogeneous drivers and parking spots of unequal attractiveness. This does not reflect the spatial and temporal heterogeneity of the parking strategies and cruising behaviours empirically evidenced by Assemi, Baker, and Paz (2020).

3. Modelling Framework

To take into account the various factors discussed in the previous section, we introduce a new modelling framework, which rests on an agent-based model with high spatial resolution. Unlike its forebears, this framework does not postulate specific behavioural rules for the drivers looking for parking. Its generic formulation opens the door to a theoretical resolution through the recourse to graph theoretical and statistical physical methods. Besides, it will allow a very efficient numerical implementation.

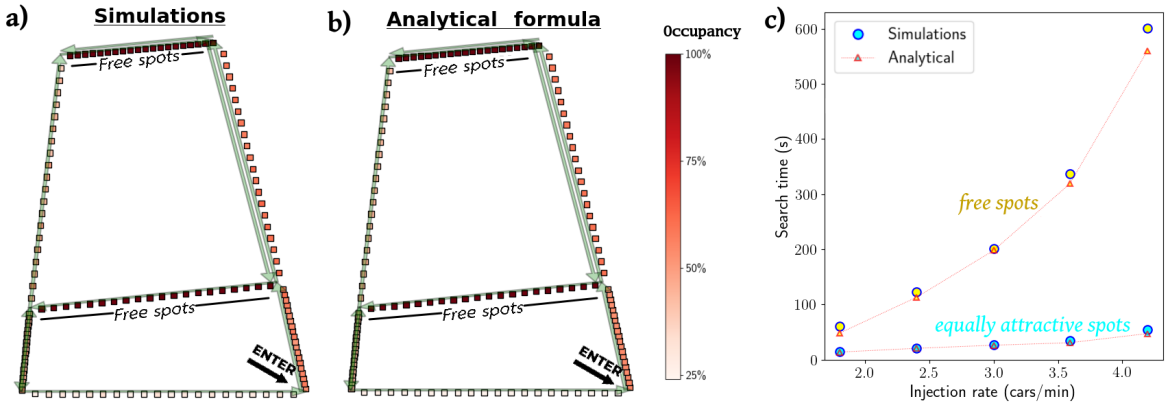

Figure 2 **Influence of the inhomogeneous attractiveness of parking spots in a small 'toy' network. Cars have equal turning probabilities at each intersection. Numerically (a) and analytically (b) derived average occupancy of parking spaces (represented as squares) in the steady state, when drivers are most attracted to free spots ($p_i = 100\%$) and only have a $p_i = 1\%$ probability to park at every other vacant spot that they drive by. Panel (c) compares the resulting mean search times with the situation in which all spots are equally attractive ($p_i = 100\%$).**

The model relies on an explicitly described network of streets (or parking alleys), with parking spots located along them. Motorists are grouped into distinct categories $\alpha = 1, 2, \ldots$ depending on their destination, trip purpose, etc. At an intersection (which is a node of the graph representing the network), they turn into an outgoing street with a probability given by the corresponding entry of the category-dependent turn-choice matrix $\underline{\underline{T}}^{(\alpha)}$. Finally, when driving by a spot i, they will choose to park there with probability $p_i^{(\alpha)}$ if it is vacant. Parked cars leave their space, and are thus removed from the simulation, at a rate $D^{(\alpha)}$, which is the reciprocal of the average parking duration.

Now, in principle, the on-site parking probability $p_i^{(\alpha)}$ depends on a variety of explanatory variables, first of which the parking rate, the distance to destination, and the odds of finding a 'better' spot estimated by the driver (Levy, Martens, and Benenson 2013, Bonsall and Palmer 2004), viz.,

$$p_i^{(\alpha)} = f(\text{rate}, \text{distance}, \ldots). \tag{1}$$

A central idea of the model is to subsume all these variables into two generic variables: (i) an attractiveness $A_i^{(\alpha)}$ reflecting how attractive a spot i is perceived to be *intrinsically* (it can estimated with surveys of stated preferences (Brooke 2016, Lee, Agdas, and Baker 2017, Antolín et al. 2018) or more recent methods based on machine-learning and the distribution of points of interest (Nie et al. 2021)), (ii) the driver's perception of how easy it currently is to park, $\beta^{(\alpha)} \in [0, \infty)$.

$$p_i^{(\alpha)}(t) = f(A_i^{(\alpha)}, \beta^{(\alpha)}(t)). \tag{2}$$

At very low occupancy, when parking seems extremely easy, viz., $\beta \to \infty$, the driver will refuse to park anywhere but in their preferred spot, of attractiveness $A_{\max}^{(\alpha)}$ (see examples in the empirical study of (Paidi et al. 2022) for example). To the opposite, at extremely high occupancy, β will tend to zero and virtually any admissible spot ($A_i^{(\alpha)} > -\infty$) may be deemed

acceptable, viz. $p_i^{(\alpha)} \to 1$. Since $p_i^{(\alpha)} \in [0,1]$, these considerations invite us to express p_i using a Boltzmann-like functional form, viz.,

$$p_i^{(\alpha)}(t) = e^{\beta^{(\alpha)}(t)\cdot(A_i^{(\alpha)} - A_{\max}^{(\alpha)})}. \tag{3}$$

At this stage, we should stress that, in practice, much will depend on the behavioural choices implicitly encoded in the attractiveness field $A_i^{(\alpha)}$ and the route choices governed by $\underline{\underline{T}}^{(\alpha)}$. Our reasoning holds for any such choices, whether they are realistic (as we claim for those made in Section 4) or not. Therefore, it reaches far beyond current studies focusing on specific rules. In this regard, let us underline that our general formulation encompasses the rules used in many previous models; Appendix A explains how these specific rules can be transcribed into our formulation.

3.1. Simplifications for the current study

Despite our wish to develop a very general model for parking, we will make a few simplifications in this first, ground-laying work.

First, while in principle each driver evaluates their own β depending on their experience along their specific trajectory, here we assume that $\beta^{(\alpha)}(t)$ only depends on the currently occupied spots in the network.

Secondly, each category of drivers will keep a constant strategy during their search. In other words, while in reality drivers may modify their turn choices and their perception of spot attractivenesses $A_i^{(\alpha)}$ over time, for instance if they see that their preferred spot is occupied, here the turning rates and attractivenesses will be prescribed once and for all, for each type of drivers. (Note, however, that the actual turn choices and parking decisions may vary due to stochasticity, in our probabilistic framework, leading to realistic circling behaviour (see Fig. 4).

Finally, for simplicity, we do not simulate cars after they have left their parking space; they will simply vanish. We should also recall that a fixed initial parking demand is considered here. Should one consider a redesign that affects the parking supply, some feedback of parking search times on the parking demand should be expected; this point will be succinctly addressed in the conclusion.

3.2. Numerical implementation

The model is implemented in C++ using data structures that lead to optimal computational performances. The nodes (i.e., intersections) and edges (i.e., street segments) of the network, and if needed the locations and attractivenesses of spots, are read from CSV files as input and used to create objects of the Spot, Node, Street, and City classes. At each time step ($dt = 1\,\mathrm{s}$ in general), a number of car objects set by a Poisson process of parameter I (where I is the global injection rate) are instantiated and injected into the network at one of the entry points. Their positions are measured relative to their current street and are updated iteratively at each time step. They switch streets upon reaching one intersection by randomly selecting an outgoing street according to the specified turning probabilities. We keep track of the (time-ordered) list of spots by which they have driven during the current time step and loop over it to test whether they have chosen to park at any of them, depending on

the attractiveness of the spot and the (constantly updated) parking tension parameter β. At each time step, another iteration over currently parked cars removes them with a probability set by their departure rate $D^{(\alpha)}$. (The numerical results shown in the previous section were obtained with this implementation.)

Let us finally underline that in our implementation each street is linked to all incoming and outgoing streets and has access to the list of spots located along it; this allows optimal computational efficiency. More details about the numerical implementation can be found in Appendix D; the C++ scripts may be shared to *academic researchers* upon reasonable request to the authors.

3.3. Mean-field analytical solution for the search time

Once thus posed, the problem is amenable to theoretical handling. Indeed, having abstracted human behaviour and strategies, we are left with the physical problem of self-propelled particles (namely, cars) moving on a directed graph (the street network) and having known probabilities to adsorb at any site (parking spot) along the edges (streets) of this graph. This does not mean in any way that the model describes motorists as brainless particles, but that these behavioural traits have been encoded into turn choices and attractiveness fields for each type of drivers, which can be processed rigorously.

From now on, it will be more convenient to consider that every street position associated with a parking spot as well as every intersection are nodes of this graph (notice that the street position where the car starts to park and the parking spot will share the same node label). The instantaneous number of cars of category α, α-cars, passing by each node per minute is then represented by a vector $\underline{I}^{(\alpha)}(t)$ of size N_{nodes}, where N_{nodes} is the number of nodes and $I_i^{(\alpha)}(t)$ is the number of cars passing by node i per minute and time t averaged over random realisations. The drivers' turn choices at the nodes define a transition matrix $\underline{\underline{T}}^{(\alpha)}$ such that $T_{ij}^{(\alpha)} \in [0,1]$ is the probability that an α-car chooses to move from node i to node j along an edge of the graph in one arbitrary time step, *if* it does not park in the meantime. In this graph theoretical approach, α-cars initially injected at nodes j (hence, $I_j^{(\alpha)}(t=0)>0$) will be found at $\underline{I}^{(\alpha)}(t=1) = \underline{I}^{(\alpha)}(0)\cdot\underline{\underline{T}}^{(\alpha)}$ at the next time step and at

$$\underline{I}^{(\alpha)}(K) = \underline{I}^{(\alpha)}(0)\cdot\left(\underline{\underline{T}}^{(\alpha)}\right)^K \tag{4}$$

after K steps, *if they do not park in the mean-time*. However, at each spot i, cars may actually have parked, with a probability $\tilde{p}_i^{(\alpha)}$ given by $\tilde{p}_i^{(\alpha)} = p_i^{(\alpha)}\,\hat{n}_i$, where $\hat{n}_i = 1-n_i$ is zero (one) if the spot is vacant (occupied). Taking this possibility to park into account, the transition matrix $\underline{\underline{T}}^{(\alpha)}$ should be replaced by $M_{ij}^{(\alpha)} = (1-\tilde{p}_i^{(\alpha)})\cdot T_{ij}^{(\alpha)}$ and the spatial distribution of cars at $t=K$ is actually

$$\underline{I}^{(\alpha)}(K) = \underline{I}^{(\alpha)}(0)\cdot\left(\underline{\underline{M}}^{(\alpha)}\right)^K. \tag{5}$$

Provided that the occupancy field (n_i) is known, the rate at which an α-car reaches spot j and parks there reads

$$P_j^{(\alpha)} = \sum_{K=0}^{\infty} I_j^{(\alpha)}(K)\cdot\tilde{p}_j^{(\alpha)}$$

$$
\begin{aligned}
&= \underline{I}^{(\alpha)}(0) \cdot \sum_{K=0}^{\infty} \left(\underline{\underline{M}}^{(\alpha)}\right)^{K} \cdot \tilde{p}_j^{(\alpha)} \\
&= \underbrace{I_i^{(\alpha)}(0)\left[\left(\underline{\underline{\mathbb{I}}} - \underline{\underline{M}}^{(\alpha)}\right)^{-1}\right]_{ij}}_{R_j^{(\alpha)}} \tilde{p}_j^{(\alpha)},
\end{aligned} \tag{6}
$$

where Einstein's summation convention (on repeated indices, excluding fixed index j here) is implied and $\underline{\underline{\mathbb{I}}}$ is the identity matrix. Here, we have considered that the occupancy field (n_i) remains unchanged during the search, which will not hold true in the regime of fierce competition between cruising cars.

Along the same lines, the average 'driving, searching, and parking' time $\mathrm{T}_s^{(\alpha,j)}$ of an α-car finally parking at spot j (in arbitrary time steps) can be derived; it is the average number of steps K needed to park at spot j, weighted by the probability $H_j^{(\alpha)}(K) \cdot \tilde{p}_j^{(\alpha)}$ to reach j after K steps and park there, where the total injection rate $I^{(\alpha)}$ of α-cars was used to non-dimensionalise $I_j^{(\alpha)}(K)$ into $H_j^{(\alpha)}(K) = I_j^{(\alpha)}(K)/I^{(\alpha)}$. Accordingly, summing over all spots j,

$$
\begin{aligned}
\mathrm{T}_s^{(\alpha)} &= \sum_{K=0}^{\infty} K \; H_i^{(\alpha)}(0) \cdot \left[\underline{\underline{M}}^{(\alpha)\,K}\right]_{ij} \cdot \tilde{p}_j^{(\alpha)} \\
&= H_i^{(\alpha)}(0) \sum_{K=0}^{\infty} \sum_{l=0}^{K-1} \cdot \left[\underline{\underline{M}}^{(\alpha)\,K}\right]_{ij} \cdot \tilde{p}_j^{(\alpha)} \\
&= H_i^{(\alpha)}(0) \cdot \sum_{l=0}^{\infty} \left[\sum_{K=l+1}^{\infty} \underline{\underline{M}}^{(\alpha)\,K}\right]_{ij} \cdot \tilde{p}_j^{(\alpha)} \\
&= H_i^{(\alpha)}(0) \cdot \sum_{l=0}^{\infty} \left[\underline{\underline{M}}^{(\alpha)\,l+1} \cdot \left(\underline{\underline{\mathbb{I}}} - \underline{\underline{M}}^{(\alpha)}\right)^{-1}\right]_{ij} \cdot \tilde{p}_j^{(\alpha)} \\
&= H_i^{(\alpha)}(0) \cdot \left[\underline{\underline{M}}^{(\alpha)} \cdot \left(\underline{\underline{\mathbb{I}}} - \underline{\underline{M}}^{(\alpha)}\right)^{-2}\right]_{ij} \cdot \tilde{p}_j^{(\alpha)}.
\end{aligned} \tag{7}
$$

Equations 6 and 7 involve matrices of linear dimension N_{nodes}, which may be very large. However, since each node is connected to a few other nodes at most, these matrices (notably $\underline{\underline{M}}^{(\alpha)}$) are particularly sparse. Therefore, their multiplication and inversion can be handled quite efficiently, for instance using the dedicated Python library (scipy.sparse); in particular, we avoid computing the inverse of sparse matrix $\underline{\underline{A}} \equiv \underline{\underline{\mathbb{I}}} - \underline{\underline{M}}^{(\alpha)}$ and, instead calculate $\underline{Y} \cdot \underline{\underline{A}}^{-1}$ by solving the linear problem $\underline{X} \cdot \underline{\underline{A}} = \underline{Y}$.

Incidentally, should an upper bound $K_{\max}$ be set on the number of steps K allowed for parking search before cars quit searching, the foregoing expressions will turn into (see Appendix B.2 for the details)

$$
\bar{P}_j^{(\alpha)} = P_j^{(\alpha)} - I_i^{(\alpha)}(0)\left[\left(\underline{\underline{\mathbb{I}}} - \underline{\underline{M}}^{(\alpha)}\right)^{-1} \cdot \underline{\underline{M}}^{(\alpha)\,K_{\max}+1}\right]_{ij} \tilde{p}_j^{(\alpha)} \tag{8}
$$

$$
\bar{\mathrm{T}}_s{}^{(\alpha)} = \mathrm{T}_s^{(\alpha)} - H_i^{(\alpha)}(0) \cdot \left[(\underline{\underline{\mathbb{I}}} - \underline{\underline{M}}^{(\alpha)})^{-2} \cdot \underline{\underline{M}}^{(\alpha)\,K_{\max}+1}\right]_{ij} \tilde{p}_j^{(\alpha)}, \tag{9}
$$

where one has arbitrarily defined as $K_{\max}$ the search time of cars that quit searching. Also note that this gives access to the survival function of the search time, that is to say, the

fraction of cars that needed longer than $K_{\max}$ steps to park, which is $\sum_j \left(P_j^{(\alpha)} - \bar{P}_j^{(\alpha)}\right)/I^{(\alpha)} = 1 - \sum_j \bar{P}_j^{(\alpha)}/I^{(\alpha)}$.

In all the above formulae, the search time was expressed in arbitrary units, each unit corresponding to the time taken for a car to travel between two nodes. To recover real time units, we introduce an auxiliary 'generating' function $\underline{\underline{N}}(z)$ defined by $N_{ij}(z) = z^{\tau_{ij}} M_{ij}^{(\alpha)}$, where z is a real variable and τ_{ij} is the travel time between neighbouring nodes i and j (note that, if i and j are not directly connected, then $M_{ij} = 0$). As with the transition matrix, exponentiating $\underline{\underline{N}}(z)$ into $\underline{\underline{N}}^K(z)$ gives access to paths of length K steps. This contrivance, detailed in Appendix B.1, helps us express the search time in real time units as

$$T_s^{(\alpha)} = H_i^{(\alpha)}(0) \cdot \left[(\underline{\underline{\mathbb{I}}} - \underline{\underline{M}}^{(\alpha)})^{-1} \cdot N'(z=1) \cdot (\underline{\underline{\mathbb{I}}} - \underline{\underline{M}}^{(\alpha)})^{-1}\right]_{ij} \tilde{p}_j^{(\alpha)}, \tag{10}$$

where the derivative of $\underline{\underline{N}}(z)$ satisfies $N'_{ij}(z=1) = \tau_{ij} M_{ij}^{(\alpha)}$

The foregoing formulae were derived for a *given* configuration of the occupancy $\underline{n}$. To get the actual *mean* search time requires averaging over an ensemble of equivalent realisations of $\underline{n}$ (or over time in the steady state). This would be straightforward if one could compute the average by plainly substituting $\langle n_j \rangle \in [0,1]$ for $n_j = 0$ or 1 in the definition of the M_{ij} matrix. Unfortunately, in general, spatio-temporal correlations between spot occupations n_i prohibit such a factorisation. Still, albeit not perfectly rigorous, this is a valid approximation in the *mean-field* regime, wherein any mutual dependence between instantaneous spot occupations is neglected. We expect it to be quite reasonable as long as the search time is not dominated by cars looping over the very same street blocks over and over again, and we thus have an equation (Eq. 10) relating the drive-and-search time to the occupancy field (n_i) in this case. Conversely, when circling starts to prevail, the approximation may lose its accuracy.

3.4. Analytical solution for the occupancy in the stationary state

Up to now, it has been assumed that the occupancy of each spot (or its time average) is known. We now purport to show that this occupancy field (n_j) can be derived theoretically, at least in some regimes. This is achieved by balancing the probability to reach a spot and park there for an incoming car with the rate of departure of a car parked at this spot. Generally speaking, the resulting equations will display a dependence on the initial occupation. In this study, we restrict our attention to the stationary state, where this dependence is washed away so that methods from steady-state statistical physics are directly applicable. In other words, in the considered time period, the parking demand is assumed to evolve slowly enough to strike a balance between incoming α-cars and departing ones, viz.,

$$0 = (1 - p_{\text{leakage}}^{(\alpha)}) I^{(\alpha)} - N \cdot \phi^{(\alpha)} \cdot D^{(\alpha)}, \tag{11}$$

where, for α-cars, the leakage fraction $p_{\text{leakage}}^{(\alpha)}$ vanishes if all incoming drivers eventually manage to park. Therefore, if only a negligible fraction of drivers quit searching, one arrives at

$$\phi^{(\alpha)} = \frac{1}{N} \cdot \frac{I^{(\alpha)}}{D^{(\alpha)}}, \tag{12}$$

and, should all categories of cars have similar parked times $1/D$,

$$\phi = \frac{1}{N} \cdot \frac{I}{D}, \tag{13}$$

where $I = \sum_\alpha I^{(\alpha)}$.

In addition to this global balance, the rate at which cars park *at any given spot* j must be balanced by the (supposedly constant) departure rate D of parked cars, viz.,

$$\sum_\alpha I^{(\alpha)} P_j^{(\alpha)} = D\langle n_j \rangle. \tag{14}$$

Using Eq. 6, one finally arrives at the mean-field stationary occupancy

$$\langle n_j \rangle = \frac{\sum_\alpha R_j^{(\alpha)} p_j^{(\alpha)} I^{(\alpha)}/D}{1 + \sum_\alpha R_j^{(\alpha)} p_j^{(\alpha)} I^{(\alpha)}/D}, \tag{15}$$

where $R_j^{(\alpha)}$, defined in Eq. 6, implicitly depends on the $\langle n_i \rangle$'s.

Note in passing that, if there is a single category of drivers, one can express p_j from Eq. 15 and, on the basis of the empirically observed occupancies $\langle n_j \rangle$, infer the *empirical attractivenesses* (or more precisely βA_j) using a fixed-point method. The problem becomes more complex in the more realistic case of multiple categories of drivers and it should be addressed in our future works.

3.5. Numerical validation of the theory on a small street network

The self-consistent formula, Eq. 15, giving the stationary mean-field occupancy is solved with the fixed-point method, using an empty network ($n_j = 10^{-5}$) as an initial guess and iteratively inserting it into Eq. 15 until the solution converges. Applied to the 'toy' network of Fig. 2(a), this method yields spot occupancies n_j that agree very well with the numerical results, as illustrated in Fig. 2(b), with a mean error per spot that does not exceed $\sim 5\%$. Using the analytical stationary occupancy, the search time in seconds is computed with the help of Eq. 10. Figure 2(c) demonstrates the excellent agreement with the simulation results, with the slight exception of the regime of harsh competition at high injection rates.

3.6. Interaction with the through-traffic

So far, the interactions between cruising cars and the underlying traffic (i.e., the outgoing and the through traffic) have been overlooked, although cruising can contribute to congestion and generate additional delays. Our framework is versatile enough to include this feedback loop with only modest changes. Indeed, as Eqs. 5 and 6 are expressed in numbers of steps K and not real time, they hold regardless of traffic-induced delays, because there is no direct competition between cruising cars under our approximations; the conservation equation, Eq. 12, also remains valid, provided that the injection rate is constant.

On the other hand, the expression for the absolute travel time, Eq. 10, must be amended because the link travel times τ_{ij} now depend on the local density k_i. Assume that the underlying traffic is known; it generates an arrival rate of $I_i^{(0)}(k_i)$ cars per hour in front of parking space i (but on the road). This rate should be added to the rate of all cruising α-cars reaching this site, $R_i^{(\alpha)}$, so that the total flow reads

$$I_i = I_i^{(0)}(k_i) + \sum_\alpha R_i^{(\alpha)}. \tag{16}$$

Our steady-state assumption implies that this traffic demand can effectively be served, i.e., I_i is lower than the peak capacity of the street link (otherwise, queues will form and diverge). Accordingly, we focus on situations with an underlying traffic that does not saturate the system's capacity, even when some cruising traffic is added to it. We can then use the fundamental diagram of the road portion to deduce from I_i the local speed, hence the actual travel time $\tau_{ij}(I_i)$ from i to j, taking due account of the underlying traffic. Finally, $\tau_{ij}(I_i)$ can be inserted into Eq. 10, where it appears in the definition of the matrix N.

Let us illustrate this method using the 'toy' network of Fig. 2 (with free spots), for an injection rate of 216 cars in search of parking per hour. For that purpose, we assume a uniform through traffic $I_i^{(0)} = 500\,\text{veh/h}$ and a flow-speed relation, say, $\text{FlowRate}(v) = 150\,(v - v^2/v_f)$ (with v in km/h and $v_f = 30\,\text{km/h}$). Using Eq. 6, we find cruising rates R_i (the α superscript has been dropped because there is just one category of drivers in that example) ranging from 26 to 240 cruising cars per hour on the different block-faces, on top of the underlying traffic, hence (from Eq. 16) total flow rates I_i of 526 to 740 cars/hour. With the proposed flow-speed relation, this results in travel times $\tau_{ij} \propto 1/v$ on the street links that are from 1% to 10% longer than without cruising traffic. (These values of τ_{ij} can be inserted into Eq. 10 to get the total driving times.)

The method could be further refined to account for the slower driving speed of cruising cars, compared to transiting ones, by introducing a dependence of the driving speed v, not on the total traffic I_i, but on *both* the underlying traffic $I^{(0)}$ and the cruising traffic. Although this refinement may be of interest in practical studies, its implementation is straightforward and will not be discussed here. In fact, in the next section, we shall neglect the contribution of the cruising traffic to congestion and consider fixed driving speeds on the street links (e.g., set by the underlying traffic), irrespective of the number of cruising cars.

3.7. Implications

The theoretical framework exposed in the previous paragraphs is somewhat technical, but it has immediate practical implications. First, it is easy to understand that, in the mean-field regime, the average parking time $1/D$ only matters relative to the parking demand quantified by the injection rates $I^{(\alpha)}$; in other words, the time unit of the problem could be reset so that $D = 1$. More importantly, these rates D and $I^{(\alpha)}$ do not directly affect the mean-field parking search time $T_s^{(\alpha)}$ (Eq. 10); their effect is mediated by the occupancy field $\underline{n}$ and the average occupancy ϕ, consistently with (Dowling, Ratliff, and Zhang 2019). This notably implies that the turnover rate, although widely believed to be central for the parking tension, only impacts the parking search process via its influence on the average occupancy. Put differently, as long as the fraction of time during which spots are occupied remains constant in a homogeneous period, increasing the turnover rate does not reduce the search time. Of course, in practice, limiting the parking time by rule or by cost *will* ease the parking pain, by altering the parking demand and the average occupancy – but not *per se*.

One should however bear in mind that these results are rigorous only under the mean-field hypothesis, which notably breaks down when drivers start circling significantly and competing for freshly vacated spots. This breakdown is particularly conspicuous in the high-occupancy (i.e., rightmost) part of Fig. 1(d) (where there is no longer a unique relation between the search time and the occupancy, especially for Parking Lot A).

4. Large-scale Application of the Method: On-street Parking in Lyon, France

So far, we have shown that our theoretical and numerical modelling framework is applicable in small-scale street networks, but its scalability to the larger-scale networks of actual cities has not been proven yet. This section is aimed at demonstrating that our methods are quite efficient in rendering parking search in a large city. It will also expose how the model can be used in practice and what input data are necessary to this end. This will be illustrated with the morning peak hour (7am to 10 am) in the city of Lyon, as of 2019, which belongs to the second urban area in France, with a municipal population around 500,000 people, and features well-known difficulties to park in its centre (SARECO / Prédit-Ademe 2005). For instance, according to 2015 household travel surveys (CEREMA 2015), 55% of the respondents with a place of work or study in Lyon mentioned parking issues and the percentage peaked at 60%-70% for those who would not drive all the way to the place of work or study. That being said, let us make it clear that our aim is not to provide the most accurate picture of parking in Lyon, which would require more input data than we own, but rather to put to the test our methods in a fairly realistic case study.

In particular, we resort to crude Origin-Destination matrices for Lyon-bound cars in the morning, on the basis of the number of people living and working in each district ('*arrondissement*'), corrected by a plainly empirical factor to reflect the proportion of drivers trying to park on the curb. Note that more accurate matrices based on GPS tracking are commercially available, but expensive. More precisely, 46 injection points ('sources') are chosen in, and at the boundary of, the city. For entry points inside the boundaries, the relative rates at which cars are injected at these points depend on the population of the *arrondissement*. For points located on the boundary, they depend on the estimated inflow of cars from outside the city. The latter points account for about half of the injected cars. The global injection rate will be varied in the following. Regarding the destinations, 36 points were selected (Fig. 3) and attract a fraction of the injected cars that is roughly proportional to the local number of jobs, upon aggregation by *arrondissement*; empirical correction factors intended to reflect the availability of private and off-street parking were introduced manually (Table S1). We assume that the injection points and the destinations are decoupled: cars are randomly bound to a destination, with the same probabilities irrespective of where it was injected. Also note that, even though our theoretical framework can include off-street parking, only drivers looking for on-street parking are considered here; parking search will therefore be described as unsuccessful if the drivers eventually opt for off-street parking or if they give up their trip altogether.

Detailed information about the locations of the $\sim$ 84,000 on-street parking spots, their rate, and their occupancy (as of 2019) as well as the street network was provided to us by the City of Lyon. Here, their attractiveness is assumed to depend exclusively on the Euclidean distance to the driver's destination and on the parking rate (either free of charge, or 1 Euro per hour or 2 Euros per hour). The hourly rate c_h in Euros is converted into an equivalent additional distance to destination $d_{\text{charge}} \approx c_h \cdot 200\,\text{m}$ by balancing the cost for a dwell time of 3 hours with the cost of walking a distance $2 \cdot d_{\text{charge}}$ (from the spot to the destination and the other way round), under the premise of a value of time around 13 Euros/h, multiplied by a penalty factor of 2 for the effort of walking (Bonsall and Palmer 2004), and an effective walking speed of 1 m/s (with respect to Euclidean distances). Finally, we consider that the attractiveness decreases with the square of the distance to destination, with a characteristic length $d_{\text{walk}} = 250\,\text{m}$, so that

$$A_i = -\frac{{d_{\text{dest}}^{(i)}}^2 + (200\,c_h)^2}{d_{\text{walk}}^2}. \tag{17}$$

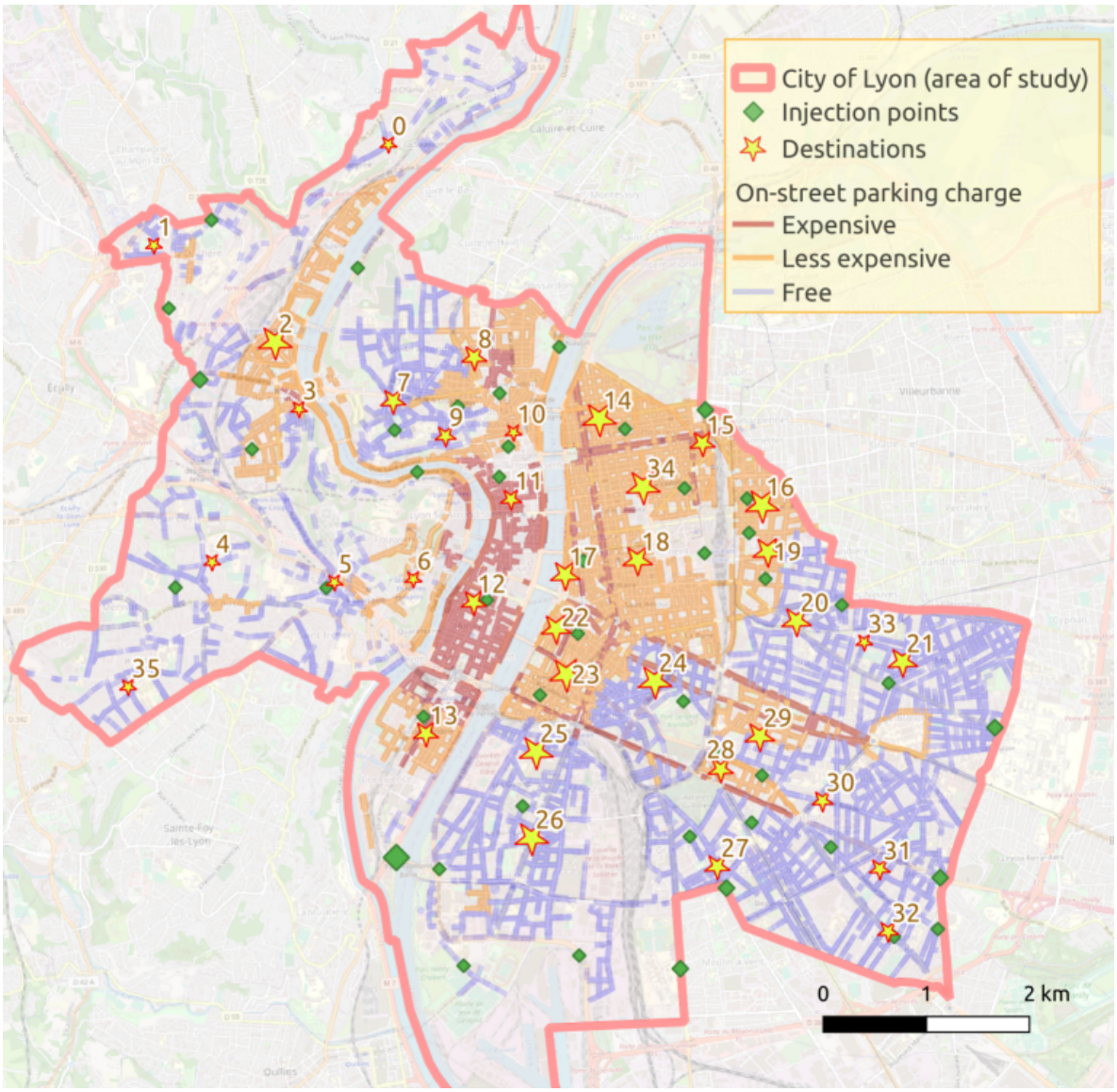

Figure 3 **Map of the city of Lyon with its 84k on-street parking spots (as of 2019) and the injection points and destinations implemented in our model (the symbol sizes represent the injection rates of cars associated with these points).**

The specific expression that we chose could be refined with targeted local phone surveys, field studies, or 'virtual experiments' (Fulman, Benenson, and Elia 2020) involving a representative panel of participants.

Regarding the perceived parking tension, we arbitrarily adopt the following expression for the dependence of the tension factor on the instantaneous local occupancy $\phi^{(\alpha)}$ (measured within a disk of radius d_{walk} around the destination), $\beta^{(\alpha)} = \frac{1-\phi^{(\alpha)}}{\phi^{(\alpha)}} + \epsilon$, where $\epsilon \ll 1$ (in practice, ϵ is set to 0.1) is introduced to prevent the selection of too distant spots at high occupancy. This assumes that the actual local occupancy close to the destination reflects the

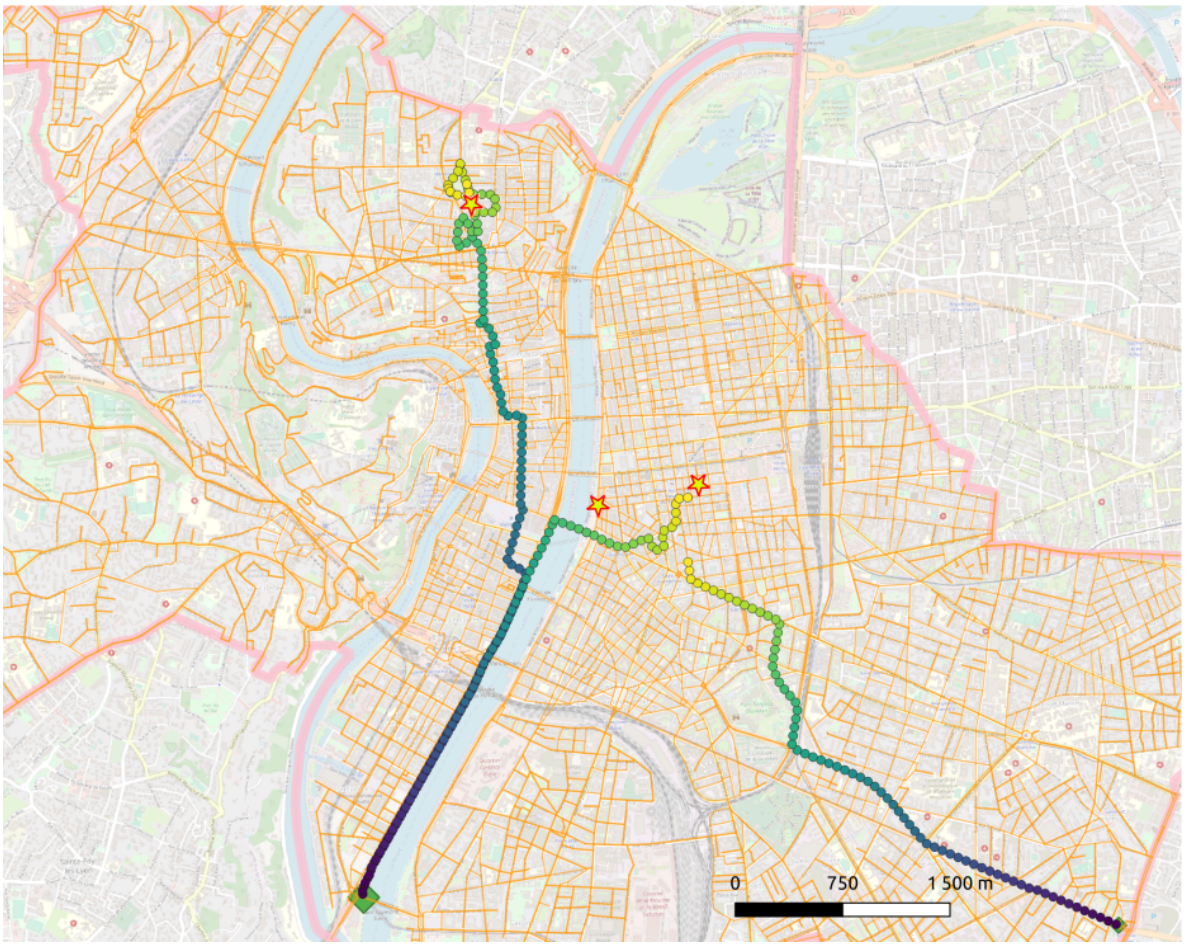

Figure 4 **Examples of a few typical simulated car trajectories, from the injection point to the parking spot near the destination, represented by a star, for a global injection rate of 50 cars/min. The colours inside the circles denote the time passed since the car's entry in the network.**

parking tension experienced by each category of users. It is noteworthy that the formula verifies $\beta^{(\alpha)} \to \epsilon \approx 0$ at very high occupancy and $\beta^{(\alpha)} \gg 1$ when $\phi^{(\alpha)}$ is small.

However, it should be realised that a large fraction of the existing spots will remain occupied over the whole simulation period (i.e., the morning peak hour). Estimating (in light of limited field data) that 95% of spots in the centre and 87% in the periphery are occupied at a given time in the morning rush hour, this long-term occupancy was replicated by randomly declaring forbidden ('frozen') a corresponding fraction of spots, reduced by 25% to 30% to account for cars departing during the simulation period. Besides, the mean parking time was set to 2.5 hours, for all destinations (note that, in any event, it cannot exceed the duration of the simulated period).

Figure 3 gives an overview of the locations and rates of parking spots, as well as the chosen injection points and destinations. Overall, cars are directed towards their target by computing the shortest-path distance $\tilde{d}$ of every node at the end of a street segment, with the help of the Dijkstra algorithm, and favouring turns into streets whose ends are closest to the destination. However, deviations from this shortest-path are allowed, all the more so

as the car gets closer to its destination. Technically, for every category α of drivers (i.e., destination), the probability of turning into an adjacent street $\mathcal{S}_i$ when a car in street $\mathcal{S}_0$ reaches an intersection is given by

$$T^{(\alpha)}_{\mathcal{S}_0\to\mathcal{S}_i} = \frac{1}{Z} e^{\eta[\tilde{d}^{(\alpha)}(\mathcal{S}_0)]\cdot\frac{\tilde{d}^{(\alpha)}(\mathcal{S}_0)-\tilde{d}^{(\alpha)}(\mathcal{S}_i)}{l_i}}, \tag{18}$$

where l_i is the length of street segment $\mathcal{S}_i$, Z is a normalising factor that makes the turning probabilities to adjacent streets sum to one, and the coefficient $\eta(\tilde{d}) = \min(5, \frac{\tilde{d}}{500\,\mathrm{m}})$ results in more deterministic trajectories far away from the destination and more fluctuations when approaching it or while cruising, where circling or spiralling behaviours are expected. We do not explicitly model the interactions with transit-related traffic and assume that cars have a constant speed $v \approx 22\,\mathrm{km/h}$ throughout the city in the morning peak hour. Typical examples of car trajectories to their parking spot, simulated with these turning probabilities, are presented in Fig. 4. One can see that the route choices to the target destination look quite reasonable and that they are possibly followed by circling in the vicinity of the destination if no attractive spot is found in the first place.

Our highly efficient computational methods enable us to simulate the driving and parking of $\sim 10^4$ cars in the whole city (containing $\sim 10^4$ street blocks) over a period of 3 hours in a matter of tens of seconds, using a single CPU core on a personal laptop. The outcome of the simulations in terms of average travel times (including parking search) is shown in Fig. 5, as a function of the global injection rate, and distinguished between destinations in Fig. 6. The excess travel time due to parking search is the difference between the observed travel time and that found for vanishing demand (injection rate). Defining the parking search time in this way circumvents the ambiguous definition of the start of the parking search or the onset of cruising, which was pointed out in (Millard-Ball, Hampshire, and Weinberger 2020).

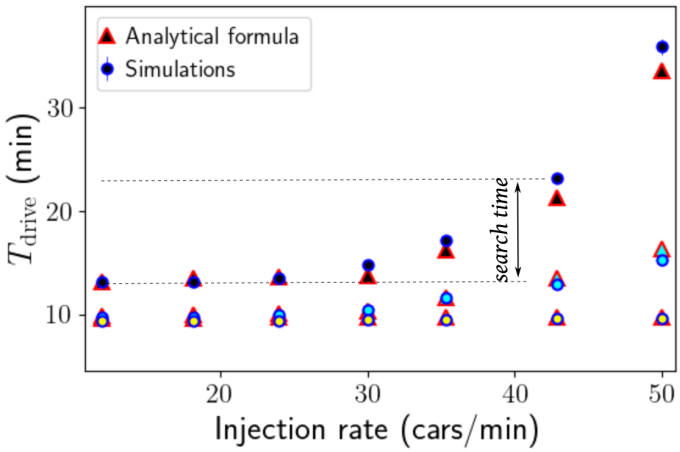

Figure 5 **Dependence of the mean total driving time, including the curbside parking search time, for two categories of drivers (i.e., two destinations, irrespective of the entry point) on the global injection rate. Black-filled symbols represent destination 10 (Cœur Croix Rousse), whereas cyan-filled and yellow-filled symbols represent destination 12 (Ainay) and destination 18 (Part-Dieu), respectively.**

Figure 5 shows that the mean search time mostly lies between a few tens of seconds and ~ 5 minutes at experimentally reasonable injection rates. Note that the search times start to

surge, although the average occupancy ϕ *over the whole city* still lies significantly below 80%. To test these results against empirical data, we have analysed the results of a massive travel survey conducted in 2015 (CEREMA 2015) in which the respondents were asked about their parking search times, among other questions. We have arrived at a mean reported search time between 2 and 3 minutes for people who parked on the curb in Lyon in the morning peak hour (the survey data contain 364 such trips), which is broadly consistent with the foregoing figures. However, we must plainly admit that we lack empirical data to rigorously gauge the accuracy of the numerical results. At best, we can say that the average search times in the simulations are reasonable and that the total travel times reported in Fig. 6 are compatible with the average time spent in trips in a day, which lies around 70 minutes in the Lyon area (Sytral / Agence d'Urbanisme aire métropolitaine Lyonnaise 2018), but this compatibility is more a safety check than a stringent validation. Furthermore, the output of the model in terms of spot occupancy is of course realistic, but this cannot be used as a touchstone, because empirical occupancy data were used as input. Lastly, the search times are found to be strongly dependent on the destination and on the injection rate, which makes sense but also urges to take with a grain of salt any empirical validation of a model based on data from a single day or place, especially if the parking demand was adjusted freely. That being said, it must not be forgotten that our goal is not to fine-tune the calibration of the model parameters to reproduce the conditions of a specific day in Lyon as closely as possible, but instead to validate the formal connections that we have established between the occupancy and the search time, as a function of the injection rate and the drivers' preferences.

Indeed, we can now make use of the theoretical arsenal introduced above to predict travel times without resorting to extensive simulations. Starting with a random initial guess for the occupancy field n_j the parking tension factors $\beta^{(\alpha)}$ are calculated based on the average local occupancies $\phi^{(\alpha)}$rmse and then serve as input for the fixed-point equation giving the occupancy field n_j, Eq. 15; the process is iterated until convergence. This occupancy field, in turn, is used to calculate the average driving time (including parking search) via Eq. 10. Figure 5 underscores the quality of these analytical predictions in the regime of low to moderate competition for spots. The analytical results also display concordance with the numerical ones if the travel times of cars are inspected separately for every destination, as shown in Fig. 6 for an injection rate of 24 cars looking for on-street parking per minute: the root-mean-square relative error on these times is smaller than 3%, while the root-mean-square absolute error on the occupancy is under 0.04 in that case. Given the complexity of the street network, the possibly intricate car trajectories (see Fig. 4), and the multiple car categories and attractiveness fields, the level of agreement displayed in Fig. 6 is remarkable. We should stress that these results were obtained using *only* the above analytical formulae, and not the output of the agent-based simulations; even the parking tension parameters $\beta^{(\alpha)}$ were determined theoretically.

Of course, besides the search times, these calculations also give access to a variety of other indicators. For instance, the total parking revenue can readily be obtained by multiplying the parking rate by the average occupancy per spot. Using the self-consistent analytical expression (Eq. 15) for the occupation number, the parking revenue generated by cars parking on the curb in Lyon in the morning peak hours is estimated at 4,720 Euros per hour (for a global injection rate of 43 cars per minute); this figure is close to the value of 4,666 Euros per hour obtained by direct numerical simulations of the model.

5. Conclusions

To summarise, our study of the parking search process has unveiled a relation between the total travel time and the occupancy of parking spaces, which takes into account the effect of

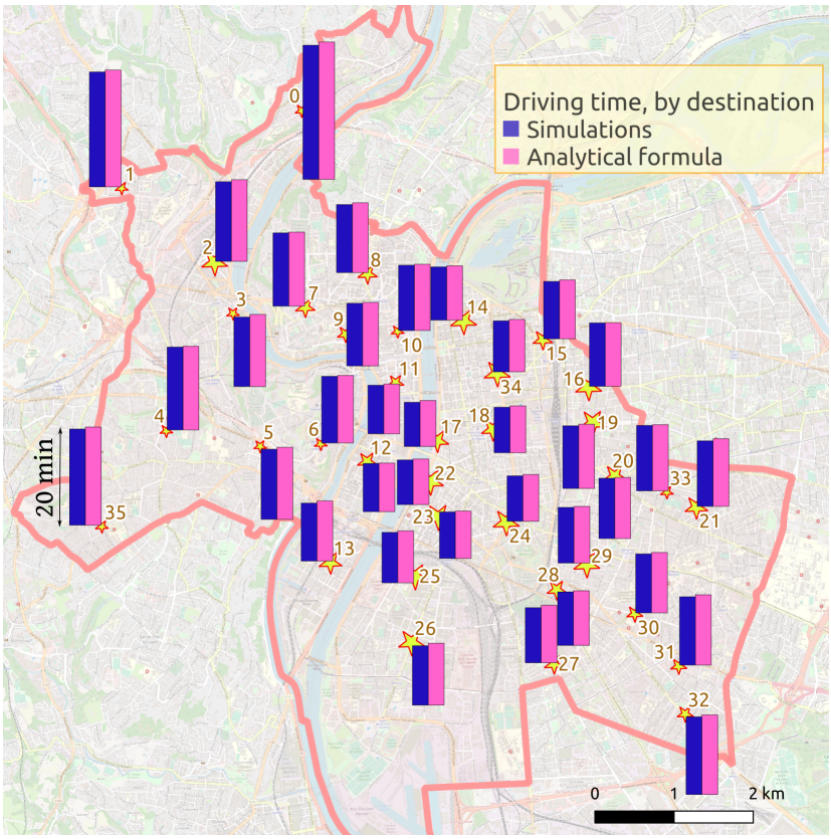

Figure 6 **Map of Lyon comparing the the simulated mean total driving time and its analytically derived counterpart for all possible destinations (drivers' category), irrespective of the entry point, for a global injection rate of 24 cars/min.**

oft-overlooked factors such as the particular topology of the street network and the heterogeneous attractiveness of parking spaces. The major contribution of this paper is to quantitatively account for these effects, inherent to the problem of parking search, by propounding an algorithm and equations of broad applicability. The derived equations are indeed generic and can therefore be applied to a wide range of parking search strategies and to any street network in the world, from simple parking lot models to large cities.

While it lays the ground for a rigorous approach to the topic, the present work involves some simplifications that limit its capacity to describe the full scope of parking-related issues. Firstly, the framework introduced here discards possible changes in behaviour of the drivers during their search (e.g., if they have a specific favourite spot and realise that it is occupied) and it handles parking decisions spot by spot, in a sequential way, overlooking the possibility to see other spots at a distance; the drivers' perception of parking tension is also handled as a function of the occupancy of the network, instead of depending on the drivers' observations. Secondly, the generic mean-field formula that we derived for the search time requires detailed information about the occupation of spots in the network; we showed how to theoretically compute such information, but only when circling remains moderate and in the stationary regime. The meaning and implications of the stationary assumption have been discussed previously; see Dowling et al. Dowling, Ratliff, and Zhang (2019).)

Still, the parallels that have been drawn with well posed physical problems (namely, the motion on a directed graph of self-propelled particles that can adsorb on its edges) bear

appealing promises: the foregoing limitations may indeed be overcome by tackling more refined physical models, which may incidentally open new avenues of research for physicists and mathematicians. Even more importantly, these abstract connections can clarify the influence of some parking characteristics on the occupancy and the search time (for instance, the parking time and the turnover rate, in this contribution).

To conclude, we would like to highlight the potential of this theoretical approach to address practically relevant issues that may be out of reach of agent-based simulations. While this study revolved around the description of a reference scenario, the formulae giving the parking search time can be integrated into a static multi-modal transport model, as part of the generalised cost of a motorised trip, in order to evaluate hypothetical scenarios of urban redesign. This would notably account for the elasticity of parking demand to search times and enable one to assess whether, for instance, reducing the parking supply increases the emission of pollutants by generating more cruising traffic or acts in the opposite way because scarcer spots and longer search times deter travelers from using their cars.

The importance of our work is even clearer if one tries to optimise some urban redesigns, which typically require numerous simulations that can be bypassed by our analytical formulae. Let us mention a few examples. One may naturally wish to restrict the parking supply while holding the cruising traffic in check. But one may also turn to adaptive parking pricing, whereby the attractiveness of spots is modulated by changing the parking rates and which has already been experimented in San Francisco and Los Angeles, notably (Shoup 2018). These modulations affect not only the demand, but also the parking search time (Dutta and Nicolas 2021); our formulae relating the search time to the attractiveness in the stationary regime can help find an optimal spatial modulation of the parking rates in busy neighbourhoods. Finally, in the context of the development of smart cities and the emergence of smart guidance and parking reservation system, our work paves the way for an assessment of the maximal performances that can be expected from smart guidance applications. This will be the focus of a forthcoming manuscript.

Acknowledgments

We thank Y. Pachot, C. Marolleau, and N. Keller-Mayaud from the City Council services of Lyon for giving us access to empirical data about parking, and Léo Bulckaen for enlightening discussions. This work was funded by an Impulsion grant from IDEXLYON (2020-2021).

Appendix A: How other agent-based models are encompassed by the proposed framework

There already exist a number of parking microsimulation models. In the main text, we have claimed that the proposed modelling framework, albeit mathematically concise, can encompass the gist of many of these models, as far as the parking search process is concerned (i.e., without considering the feedback loop of parking search on the parking demand, which pertains to the higher-level transport model into which our parking model can be integrated). This section supports this statement.

Let us start with the recent PARKGRID model described in Fulman and Benenson (2021), in which agents are injected into a grid-like city with a Poisson rate of injection (as in our case). They start

searching a parking space within 500 m of their destination, driving along street links and parking in the first available space, regardless of the parking rate. In our framework, this means that all spots within 500 m of the destination have the same attractiveness $A_i = 0$ and the other ones have an attractiveness $A_i \to -\infty$. If drivers reach the end of the street link before finding a vacant spot, they will turn to an adjacent link with probabilities set according to the results of earlier virtual experiments similar to those in Fulman, Benenson, and Elia (2020). These probabilities can straightforwardly be encoded in our matrix of turning probabilities $\underline{\underline{T}}$. Finally, if they fail to park after 20 minutes, they stop searching for on-street parking, which is equivalent to setting our upper bound for the parking search time to 20 minutes. Accordingly, the foregoing rules can naturally be described within our framework. Note, however, that this paper assumes a uniform distribution of parking times, whereas we considered a constant departure rate here.

Turning to PARKAGENT (Benenson, Martens, and Birfir 2008), the route choice is simpler in this model, insofar as drivers choose the street segment that brings them closest to their destination, which can of course also be encoded in our turn-choice matrix. They start searching for parking when they are within a distance of 100 m (rather than 500 m) of the destination and reduce their driving speed to do so, which can be implemented in our model (because driving speeds on street links may vary with the category of drivers), although we have not done it in our test studies. But interestingly they do not necessarily park in the first vacant spot. Instead, they assess the odds of finding a vacant spot before the destination, on the basis of the percentage p_{unocc} of vacant spots among those that they have seen so far and the estimated number N_s of spots to be encountered before reaching the destination. Taking this into account, they will accept a spot with probability $\max[0, \min(1, 1.5 - 0.5 * p_{\mathrm{unocc}} \cdot N_s)]$. In our model, this can approximately be transcribed by setting $\beta^{(\alpha)} = 1 - \phi \approx p_{\mathrm{unocc}}$ (where ϕ is the occupancy) and A_i equal to 1.5 times the negative of the distance from spot i to the destination, measured in number of spots, if one accepts that $e^{-1.5x}$ is of order 1 for $x < 1$ and much smaller than 1 for $x > 3$. Nevertheless, note that in this formula the percentage of vacant spots is assessed based on the actual occupancy ϕ, and not the user's estimate p_{unocc}, which we cannot transcribe in our model. If drivers have failed to park before reaching their destination, they will park in the first vacant spot within a disk whose radius grows with time. The new strategy is tantamount to setting A_i to 0 or $-\infty$ depending on the distance from spot i to the destination, as in PARKGRID, but so far we have not implemented the possibility of changes in parking strategies over time. Still, the change in strategy should be of little importance in the simulations, because the specified route choices appear to maintain the driver close to the destination, where the probability to accept a vacant spot is very high. Finally, drivers consider the search unsuccessful after 10 minutes, rather than the aforementioned 20 minutes in PARKGRID.

The SUSTAPARK model Dieussaert et al. (2009) hinges on a discrete-choice model (with logit probabilities) for the choice of a parking mode (on-street, private, or garage) and also for the probability

p_i to accept a vacant on-street parking space. The utility U_i of the latter is a linear combination intrinsic characteristics of the spot, to which a term describing the occupancy ϕ_{street} in the street is added. The resulting parking acceptance probability $p_i = \frac{1}{1+e^{-\beta_\phi \phi_{\text{street}}} e^{-U_i}}$ can be recast into the general form of Eq. 2, but not into the Boltzmann-like form of Eq. 3. However, the methodology exposed in Sec. 3.3 does not rely on this functional form and is therefore still applicable. On the other hand, our model was only applied to on-street parking; it does not describe the changes in parking mode implemented in SUSTAPARK. Finally, drivers follow random routes close to their destination, which can be encoded in our turn-choice matrix, but drivers change their speed when they start searching for parking.

Axhausen et al.'s microsimulation introduced in Horni et al. (2013) in view of an integration in MATSim also considers different parking strategies, but it presents specific features for the search process. First, agents may either drive directly to the destination and start searching from there, or start their search a given distance away from it. An easy way to take this into account in our analytical derivation is to consider that the agents are injected at the position where they start searching for parking. Drivers then accept a parking space depending on its distance to destination (as in our model), but also on the elapsed search time. This specific feature, which introduces a dependence on the driver's history, cannot be accurately replicated by our approach. Still, on a more *qualitative* level, our parking tension parameter β has the same effect as the elapsed search time: parking acceptance will be enhanced by both of these variables. Regarding route choices, they are determined probabilistically once the search has begun, which is compatible with our approach.

Finally, the approach most closely related to our model is probability the network of finite-capacity queues introduced by Ratliff et al. (2016), Dowling, Ratliff, and Zhang (2019), and Tavafoghi, Poolla, and Varaiya (2019), in that it also involves analytical developments; this elegant approach was employed to address the problem of estimating the cruising traffic on the basis of empirical occupancy data (Dowling, Ratliff, and Zhang 2019). In the model, street segments are block-faces on a Manhattan-city grid and each one of them is handled as a finite-capacity queue that serves the driver if it contains a vacant space, or rejects it to adjacent block-faces otherwise. We note that, compared to ours, this model rests on the following additional assumptions:

(i) drivers at junction select the next street segment purely randomly and the nodes of the street network only differ by their degree,

(ii) every agent will accept the first vacant space they encounter (which translates into a uniform attractiveness field in our model),

(iii) adjacent block-faces have similar levels of occupancy.

Appendix B: Details pertaining to the Analytical Calculations

B.1. Search time in real time units

In the main text, we have exposed the calculation of the search time expressed in arbitrary units (Eq. 7). To do so, drivers were split into distinct categories α, each endowed with their own matrix of turning probabilities $\underline{\underline{T}}^{(\alpha)}$ and generalised transition matrix $M_{ij}^{(\alpha)} = (1 - p_i^{(\alpha)}\,\hat{n}_i)\cdot T_{ij}^{(\alpha)}$. Since ${M^{(\alpha)}}^K$ determines how the density of cars evolves on the graph in K steps (i.e., hops from node to node), we were able to calculate the average number of steps before parking.

In order to derive a search time in minutes, a slightly more elaborate method is needed. For that purpose, we insert the transition matrix into a 'generating' function $z \to \underline{\underline{N}}^{(\alpha)}(z)$, where z is a real variable, $N_{ij}^{(\alpha)}(z) = z^{\tau_{ij}}\, M_{ij}^{(\alpha)}$, and τ_{ij} is the travel time from node i to node j. At this stage, one can notice that the exponentiation of this matrix to the power K yields

$$\left[\underline{\underline{N}}^{(\alpha)^K}\right]_{ij}(z) = \sum_{\pi\,\mathrm{s.t.}\,\pi_0=0,\pi_K=j} z^{\tau_{\pi_0\pi_1}+\ldots+\tau_{\pi_{K-1}\pi_K}} \prod_{k=0}^{K-1} M_{\pi_k\pi_{k+1}}, \tag{S1}$$

where the sum runs over permutations π of indices (or 'paths') such that $\pi_0 = i$ and $\pi_K = j$. It immediately follows that

$$\frac{d}{dz}\left[\underline{\underline{N}}^{(\alpha)^K}\right]_{ij}(z=1) = \sum_{\pi\,\mathrm{s.t.}\,\pi_0=0,\pi_K=j} \left(\tau_{\pi_0\pi_1}+\ldots+\tau_{\pi_{K-1}\pi_K}\right) \prod_{k=0}^{K-1} M_{\pi_k\pi_{k+1}} \tag{S2}$$

is the probability to reach spot j a number K of steps after injection of the car at node i, multiplied by the total travel time from i to j. The (unbound) travel time before parking thus reads

$$\begin{aligned} T_s^{(\alpha)} &= H_i^{(\alpha)}(0)\cdot \sum_{K=0}^{\infty} \frac{d}{dz}\left[\underline{\underline{N}}^{(\alpha)^K}\right]_{ij}(z=1)\cdot \tilde{p}_j^{(\alpha)} \\ &= H_i^{(\alpha)}(0)\cdot \frac{d}{dz}\left[\left(\underline{\underline{\mathbb{I}}} - \underline{\underline{N}}^{(\alpha)}(z)\right)^{-1}\right]_{ij}(z=1)\cdot \tilde{p}_j^{(\alpha)} \end{aligned}$$

But, since $\frac{d\underline{\underline{A}}^{-1}}{dz} = -\underline{\underline{A}}^{-1}(z)\frac{d\underline{\underline{A}}}{dz}\underline{\underline{A}}^{-1}(z)$ for any differentiable function $z \to \underline{\underline{A}}(z)$ of invertible matrices $\underline{\underline{A}}(z)$ and $\underline{\underline{N}}^{(\alpha)}(z=1) = \underline{\underline{M}}^{(\alpha)}$,

$$T_s^{(\alpha)} = H_i^{(\alpha)}(0)\cdot \left[\left(\underline{\underline{\mathbb{I}}} - \underline{\underline{M}}^{(\alpha)}\right)^{-1}\cdot \underline{\underline{N}}^{(\alpha)\prime}(z=1)\cdot \left(\underline{\underline{\mathbb{I}}} - \underline{\underline{M}}^{(\alpha)}\right)^{-1}\right]_{ij}\cdot \tilde{p}_j^{(\alpha)}, \tag{S3}$$

where we recall that $N_{ij}^{(\alpha)\prime}(z=1) = \tau_{ij} M_{ij}^{(\alpha)}$ and $\tilde{p}_j^{(\alpha)} = \hat{n}_j p_j^{(\alpha)}$.

Equation S3 expresses the mean search time in minutes (or, more generally, in the same units as τ_{ij}) as a function of the occupancy field (n_j).

B.2. Capped search time in arbitrary and real time units

Equations 6 and 7 of the main text give the mean search time of drivers that will hypothetically keep cruising forever. In reality, one expects them to quit searching after a given time.

Let us first assume that this upper time bound is given as a number $K_{\max}$ of steps from node to node. Then, capping the search simply implies restricting the sum on K in Eqs 6 and 7 to $0 \leqslant K \leqslant K_{\max}$, which yields Eq. 8 for the probability $\bar{P}_j^{(\alpha)}$ to reach spot j and park there. The stationary occupancy field (n_j) can then be derived iteratively by inserting the capped reaching probabilities $\bar{R}_j^{(\alpha)} \equiv \bar{P}_j^{(\alpha)}/\tilde{p}_j$ into Eq. 15.

Once the occupancy field is known, one can turn to the capped search time expressed as a number of steps,

$$\begin{aligned}
\bar{\mathrm{T}}_s{}^{(\alpha)} &= H_i^{(\alpha)}(0) \cdot \left[\sum_{K=0}^{K_{\max}} K \, \underline{\underline{M}}^{(\alpha)\,K} + \sum_{K=K_{\max}+1}^{\infty} K_{\max} \, \underline{\underline{M}}^{(\alpha)\,K} \right]_{ij} \tilde{p}_j^{(\alpha)} \\
&= H_i^{(\alpha)}(0) \cdot \left[\sum_{K=0}^{K_{\max}} K \, \underline{\underline{M}}^{(\alpha)\,K} + K_{\max} \left(\underline{\underline{\mathbb{I}}} - \underline{\underline{M}}^{(\alpha)} \right)^{-1} \cdot \underline{\underline{M}}^{(\alpha)\,K_{\max}+1} \right]_{ij} \tilde{p}_j^{(\alpha)} \\
&= H_i^{(\alpha)}(0) \cdot \left[\sum_{K=0}^{K_{\max}} \sum_{l=0}^{K-1} \underline{\underline{M}}^{(\alpha)\,K} + K_{\max} \left(\underline{\underline{\mathbb{I}}} - \underline{\underline{M}}^{(\alpha)} \right)^{-1} \cdot \underline{\underline{M}}^{(\alpha)\,K_{\max}+1} \right]_{ij} \tilde{p}_j^{(\alpha)},
\end{aligned}$$

where one has arbitrarily defined as $K_{\max}$ the search time of cars that quit searching.

Using the following identity,

$$\begin{aligned}
\sum_{K=0}^{K_{\max}} \sum_{l=0}^{K-1} \underline{\underline{M}}^{(\alpha)\,K} &= \sum_{l=0}^{K_{\max}-1} \sum_{K=l+1}^{K_{\max}} M^K \\
&= (\underline{\underline{\mathbb{I}}} - \underline{\underline{M}}^{(\alpha)})^{-1} \sum_{l=0}^{K-1} \underline{\underline{M}}^{(\alpha)\,l+1} \left(\underline{\underline{\mathbb{I}}} - \underline{\underline{M}}^{(\alpha)\,K_{\max}-l} \right) \\
&= \underline{\underline{M}}^{(\alpha)} \cdot (\underline{\underline{\mathbb{I}}} - \underline{\underline{M}}^{(\alpha)})^{-2} \cdot (\underline{\underline{\mathbb{I}}} - \underline{\underline{M}}^{(\alpha)\,K_{\max}}) - K_{\max} (\underline{\underline{\mathbb{I}}} - \underline{\underline{M}}^{(\alpha)})^{-1} \cdot \underline{\underline{M}}^{(\alpha)\,K_{\max}+1},
\end{aligned}$$

we arrive at

$$\begin{aligned}
\bar{\mathrm{T}}_s{}^{(\alpha)} &= H_i^{(\alpha)}(0) \cdot \left[\underline{\underline{M}}^{(\alpha)} \cdot (\underline{\underline{\mathbb{I}}} - \underline{\underline{M}}^{(\alpha)})^{-2} \cdot (\underline{\underline{\mathbb{I}}} - \underline{\underline{M}}^{(\alpha)\,K_{\max}}) \right]_{ij} \tilde{p}_j^{(\alpha)} \\
&= \mathrm{T}_s^{(\alpha)} - H_i^{(\alpha)}(0) \cdot \left[(\underline{\underline{\mathbb{I}}} - \underline{\underline{M}}^{(\alpha)})^{-2} \cdot \underline{\underline{M}}^{(\alpha)\,K_{\max}+1} \right]_{ij} \tilde{p}_j^{(\alpha)}.
\end{aligned} \tag{S4}$$

As in the main text, Einstein's summation convention on repeated indices is implied.

To recover real time units, we calculate an average conversion factor between steps K and seconds using the case of unbound searches, by equating the (unbound) search time given by Eq. 7 and that

given by Eq. 10. The maximum number of steps $K_{\max}$ is then first estimated from the maximum allowed time and the capped search time $\bar{\mathrm{T}}_s^{(\alpha)}$ is eventually converted into seconds on the same basis.

Unfortunately, evaluating the capped search time via Eq. S4 involves the computation of $\underline{\underline{M}}^{(\alpha)\,K_{\max}+1}$ for $K_{\max} \gg 1$, which will not necessarily be a sparse matrix even if $\underline{\underline{M}}^{(\alpha)}$ is. This computation turns out to be numerically very demanding if the number of nodes in the graph is huge, as in the Lyon test case. However, the method is operational and quick on smaller networks. Consider for example the 'toy' network introduced in Fig. 2(a). Capping search times to 180 s reduces the simulated mean search time all the more as the injected rate is high, as expected and shown on Fig. S1. These capped times are very well captured by the theoretical method outlined above, culminating in Eq. S4, as can be seen on Fig. S1.

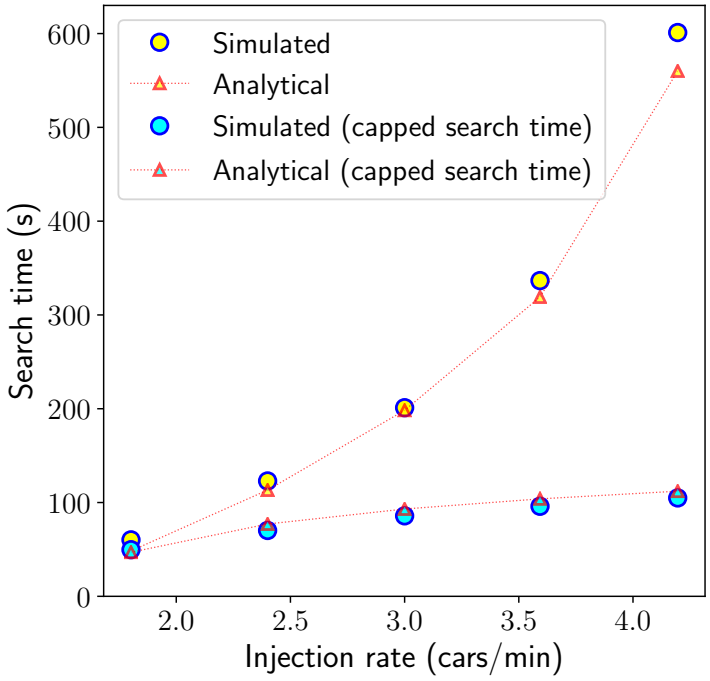

Figure S1 **Variations of the driving and cruising time in the 'toy' network of Fig. 2(a) (with free spots) with the car injection rate. The outcome of the simulation (circles) is compared with the analytical predictions (triangles), both in the case of unbound search times and when search times are capped to** 180 s.

Appendix C: Detailed Input for the Simulations of Lyon

Section 4 presented a large-scale application of the proposed framework in the case of the city of Lyon, France. In this application, drivers are classified into 36 categories according to their final destination (the list of which is given in Tab. S1). Their cars are injected into the networks at one of the 49 entry

points enumerated in Tab. S3, with a relative probability inferred either from the population of the surrounding neighbourhood or on a rough estimation of the inflow from the periphery of the city, if the entry point is located at its boundary.

Label	Name	x	y	Probability
0	Saint-Rambert - industrie	841367.9	6523437.7	0.013
1	La Duchère	839095.5	6522460.5	0.009
2	Vaise	840269.9	6521523.7	0.047
3	Champvert – Point-du-jour	840501.8	6520877.9	0.016
4	Ménival - La Plaine	839660	6519395.7	0.012
5	Saint-Just	840845.5	6519201.4	0.012
6	Vieux-Lyon	841609.7	6519231.4	0.012
7	Chazière -Flammarion	841413.3	6520955.4	0.028
8	Cœur Croix-Rousse	842199.3	6521377.5	0.028
9	Les Chartreux	841921.4	6520617	0.018
10	Pentes	842580	6520652.1	0.013
11	Terreaux – Cordeliers	842555.7	6520004.7	0.019
12	Ainay	842195	6519007.4	0.026
13	Sud Perrache	841731.4	6517736.3	0.031
14	Tête d'or – Foch	843412.4	6520782.8	0.04
15	Brotteaux – Europe	844411.3	6520546.7	0.028
16	Bellecombe – Thiers	844989.5	6519947.4	0.041
17	Mutualité-Préfecture	843080.8	6519272	0.032
18	Part-Dieu - Bir Hakeim	843782.1	6519416.5	0.032
19	Paul Bert – Villette	845042.8	6519497.8	0.036
20	Dauphiné - Sans Souci	845321.7	6518826.4	0.032
21	Montchat	846350.6	6518432.2	0.032
22	Jean Macé	842992.7	6518754.3	0.037
23	Guillotière	843092.8	6518310.3	0.047
24	Blandan	843950.4	6518243.7	0.047
25	Gerland nord	842799.7	6517560.4	0.047
26	Gerland sud	842756.2	6516727.5	0.047
27	Grand Trou – Moulin à vent	844554.8	6516452.7	0.027
28	Monplaisir	844588.2	6517391.2	0.027
29	Le Bachut	844966.5	6517711.6	0.036
30	Etats-Unis	845574.1	6517087.7	0.023
31	Mermoz – Laennec	846128.7	6516429	0.022
32	Général André - Santy	846210.7	6515824.3	0.022
33	Pinel	845979	6518623	0.014
34	6e arrondissement Sud	843836.9	6520125.1	0.040
35	5e arrondissement Sud	838846.3	6518189.5	0.012

Table S1 List of the 36 destinations implemented in our study of Lyon. The 'probability' column specifies the fraction of cars bound to a given destination. Coordinates are given in the RGF-93/Lambert-93 reference system.

Label	x	y	Proba of injection $I_i(0)$
0	843661	6520685	0.017
1	841446	6516539	0.161
2	844237	6520113	0.017
3	840046	6520488	0.024
4	842098	6515492	0.011
5	846715	6516345	0.048
6	846268	6515772	0.012
7	843023	6521479	0.017
8	841709	6517901	0.014
9	844843	6520013	0.017
10	846215	6518226	0.020
11	843218	6515591	0.011
12	844862	6519680	0.020
13	842529	6520514	0.007
14	844989	6517334	0.012
15	839541	6521161	0.064
17	842670	6517036	0.011
18	844226	6518050	0.011
20	841862	6516427	0.011
21	841071	6522242	0.017
22	847245	6517797	0.039
23	841429	6520673	0.007
24	844289	6516742	0.012
25	842837	6518111	0.011
26	842041	6520903	0.007
27	839305	6519151	0.012
28	839305	6519151	0.012
29	841647	6520269	0.012
30	845762	6518982	0.023
31	839240	6521852	0.024
32	846693	6515848	0.012
33	844198	6515464	0.048
34	843204	6518705	0.011
35	844645	6516244	0.048
36	840767	6519147	0.012
38	845656	6516640	0.012
39	843257	6519411	0.020
40	844439	6520869	0.042
41	844554	6517528	0.012
42	844889	6516878	0.012
43	842446	6521030	0.007
44	844431	6519483	0.020
45	845021	6519236	0.020
47	842325	6519031	0.015
48	839654	6522705	0.023

Table S3 List of the 49 entry points considered for the injection of cars into the street network, with their relative probabilities. Coordinates are given in the RGF-93/Lambert-93 reference system.

Appendix D: Numerical Implementation of the Agent-based Model

The numerical implementation of the agent-based model relies on the C++ classes:

City
Attributes: name, number of car categories, list of streets, list of nodes, matrices of turn-choices for all car categories, list of active cars, list of parked cars, various storage vectors

Street
Attributes: name, identifier, start and end nodes, number of spots, length, effective speed, various storage vectors

Node
Attributes: identifier, GPS coordinates, lists of incoming and outgoing streets

Spot
Attributes: (inherits from Node), identifier, vacancy status, attractiveness, various storage vectors

Car
Attributes: car number, car type, car status (active, searching for parking, parked, frozen, exited), destination, beta, position (on street or spot), matrix of turn-choices, various timestamps.

The main loop of the script runs as explained in Alg. 1 in pseudo-code:

Algorithm 1 Main loop

for t in all time steps ($dt = 1\,\mathrm{s}$) **do**
- draw number of new cars to be injected from a Poisson distribution
- **for** car in cars to be injected **do**
  - compute the normalized cumulative distribution function (cdf) of all probabilities at all possible injection nodes
  - select an injection node among the possibilities by mapping a random number onto the interval of the computed cdf
  - inject the car at the chosen node
- **end for**
- **for** car in active cars **do**
  - update the perceived tension β
  - **while** current timestep is not over **do**
    - move the car so far as possible along current street
    - store in a list L_{spots} the spots by which the car has driven
    - compute cumulative distribution function (cdf) of probabilities of all possible parking choices in L_{spots} based on attractiveness
    - **for** spot in L_{spots} **do**
      - decide if car parks here by mapping a random number on the interval of the computed cdf
      - **if** car parks here **then**
        - end 'WHILE' loop
      - **end if**
    - **end for**
    - **if** car has reached end of street **then**
      - compute the cdf of probabilities of all possible transitions available from the node at the end of street
      - select the outgoing street in which to move the car in the usual way
      - move the car into next street
    - **end if**
    - record car position
    - update leftover time in current timestep
  - **end while**
- **end for**
- **for** car in parked cars **do**
  - compute departure rate
  - randomly decide if car is removed (departs)
- **end for**
- keep track of the global balance of injected, active, parked and departed cars

end for

References

Al-Turjman F, Malekloo A, 2019 *Smart parking in iot-enabled cities: A survey. Sustainable Cities and Society* 49:101608.

Anderson SP, De Palma A, 2004 *The economics of pricing parking. Journal of urban economics* 55(1):1–20.

Antolín G, Ibeas Á, Alonso B, dell'Olio L, 2018 *Modelling parking behaviour considering users heterogeneities. Transport Policy* 67:23–30.

Arnott R, Williams P, 2017 *Cruising for parking around a circle. Transportation research part B: methodological* 104:357–375.

Assemi B, Baker D, Paz A, 2020 *Searching for on-street parking: an empirical investigation of the factors influencing cruise time. Transport Policy* 97:186–196.

Axhausen KW, Polak JW, Boltze M, Puzicha J, 1994 *Effectiveness of the parking guidance information system in frankfurt am main. Traffic engineering & control* 35(5):304–309.

Belloche S, 2015 *On-street parking search time modelling and validation with survey-based data. Transportation Research Procedia* 6:313–324.

Benenson I, Martens K, Birfir S, 2008 *Parkagent: An agent-based model of parking in the city. Computers, Environment and Urban Systems* 32(6):431–439.

Bonsall P, Palmer I, 2004 *Modelling drivers' car parking behaviour using data from a travel choice simulator. Transportation Research Part C: Emerging Technologies* 12(5):321–347.

Boujnah H, 2017 *Modélisation et simulation du système de stationnement pour la planification de la mobilité urbaine: application au territoire de la cité Descartes*. Ph.D. thesis, Paris Est.

Brooke S, 2016 *Factors influencing urban on-street parking search time using a multilevel modelling approach*. Ph.D. thesis, Loughborough University.

Brooke S, Ison S, Quddus M, 2014 *On-street parking search: review and future research direction. Transportation Research Record* 2469(1):65–75.

Cao J, Menendez M, 2015 *System dynamics of urban traffic based on its parking-related-states. Transportation Research Part B: Methodological* 81:718–736.

CEREMA, 2015 *Enquête ménages déplacements (EMD), Lyon / Aire métropolitaine lyonnaise*. ADISP (broadcaster).

Chatman DG, Manville M, 2014 *Theory versus implementation in congestion-priced parking: An evaluation of sfpark, 2011–2012. Research in Transportation Economics* 44:52–60.

Cookson G, Pishue B, 2017 *The impact of parking pain in the us, uk and germany*. Technical report, INRIX.

Dieussaert K, Aerts K, Steenberghen T, Maerivoet S, Spitaels K, 2009 *Sustapark: an agent-based model for simulating parking search. AGILE International Conference on Geographic Information Science, Hannover*, 1–11.

Dowling CP, Ratliff LJ, Zhang B, 2019 *Modeling curbside parking as a network of finite capacity queues. IEEE Transactions on Intelligent Transportation Systems* 21(3):1011–1022.

Dutta N, Nicolas A, 2021 *Searching for parking in a busy downtown district: An agent-based computational and analytical model. 2021 International Symposium on Computer Science and Intelligent Controls (ISCSIC)*, 348–354 (IEEE).

Fulman N, Benenson I, 2021 *Approximation method for estimating search times for on-street parking. Transportation Science* .

Fulman N, Benenson I, Elia EB, 2020 *Modeling parking search behavior in the city center: A game-based approach. Transportation Research Part C: Emerging Technologies* 120:102800.

Gallo M, D'Acierno L, Montella B, 2011 *A multilayer model to simulate cruising for parking in urban areas. Transport policy* 18(5):735–744.

Gao H, Yun Q, Ran R, Ma J, 2021 *Smartphone-based parking guidance algorithm and implementation. Journal of Intelligent Transportation Systems* 1–17.

Geroliminis N, 2015 *Cruising-for-parking in congested cities with an mfd representation. Economics of Transportation* 4(3):156–165.

Gu Z, Najmi A, Saberi M, Liu W, Rashidi TH, 2020 *Macroscopic parking dynamics modeling and optimal real-time pricing considering cruising-for-parking. Transportation Research Part C: Emerging Technologies* 118:102714.

Hampshire RC, Jordon D, Akinbola O, Richardson K, Weinberger R, Millard-Ball A, Karlin-Resnik J, 2016 *Analysis of parking search behavior with video from naturalistic driving. Transportation Research Record* 2543(1):152–158.

Hampshire RC, Shoup D, 2018 *What share of traffic is cruising for parking? Journal of Transport Economics and Policy (JTEP)* 52(3):184–201.

Horni A, Montini L, Waraich RA, Axhausen KW, 2013 *An agent-based cellular automaton cruising-for-parking simulation. Transportation Letters* 5(4):167–175.

Krapivsky P, Redner S, 2019 *Simple parking strategies. Journal of Statistical Mechanics: Theory and Experiment* 2019(9):093404.

Krapivsky P, Redner S, 2020 *Where should you park your car? the rule. Journal of Statistical Mechanics: Theory and Experiment* 2020(7):073404.

Leclercq L, Sénécat A, Mariotte G, 2017 *Dynamic macroscopic simulation of on-street parking search: A trip-based approach. Transportation Research Part B: Methodological* 101:268–282.

Lee J, Agdas D, Baker D, 2017 *Cruising for parking: New empirical evidence and influential factors on cruising time. Journal of Transport and Land use* 10(1):931–943.

Lehner S, Peer S, 2019 *The price elasticity of parking: a meta-analysis. Transportation Research Part A: Policy and Practice* 121:177–191.

Levy N, Martens K, Benenson I, 2013 *Exploring cruising using agent-based and analytical models of parking. Transportmetrica A: Transport Science* 9(9):773–797.

Mantouka EG, Fafoutellis P, Vlahogianni EI, 2021 *Deep survival analysis of searching for on-street parking in urban areas. Transportation Research Part C: Emerging Technologies* 128:103173.

Millard-Ball A, Hampshire RC, Weinberger R, 2020 *Parking behaviour: The curious lack of cruising for parking in san francisco. Land Use Policy* 91:103918.

Nie Y, Yang W, Chen Z, Lu N, Huang L, Huang H, 2021 *Public curb parking demand estimation with poi distribution. IEEE Transactions on Intelligent Transportation Systems* 23(5):4614–4624.

Paidi V, Håkansson J, Fleyeh H, Nyberg RG, 2022 *Co2 emissions induced by vehicles cruising for empty parking spaces in an open parking lot. Sustainability* 14(7):3742.

Polak J, Axhausen KW, 1990 *Parking search behaviour: A review of current research and future prospects. Transport Studies Units, Working Paper* 540.

Ratliff LJ, Dowling C, Mazumdar E, Zhang B, 2016 *To observe or not to observe: Queuing game framework for urban parking. 2016 IEEE 55th Conference on Decision and Control (CDC)*, 5286–5291 (IEEE).

SARECO / Prédit-Ademe, 2005 *Le temps de recherche de stationnement.* Technical report, SARECO / Prédit-Ademe.

Schadschneider A, Chowdhury D, Nishinari K, 2010 *Stochastic transport in complex systems: from molecules to vehicles* (Elsevier).

Shoup D, 2018 *Parking and the City* (Routledge).

Shoup DC, 2006 *Cruising for parking. Transport policy* 13(6):479–486.

Sytral / Agence d'Urbanisme aire métropolitaine Lyonnaise, 2018 *Pratiques de déplacements sur les bassins de vie du scot de l'agglomération lyonnaise (2015).* Technical report, Sytral / Agence d'Urbanisme aire métropolitaine Lyonnaise.

Tanaka S, Ohno S, Nakamura F, 2017 *Analysis on drivers' parking lot choice behaviors in expressway rest area. Transportation research procedia* 25:1342–1351.

Tavafoghi H, Poolla K, Varaiya P, 2019 *A queuing approach to parking: Modeling, verification, and prediction. arXiv preprint arXiv:1908.11479* .

Vo TTA, van der Waerden P, Wets G, 2016 *Micro-simulation of car drivers' movements at parking lots. Procedia Engineering* 142:100–107.

Weinberger RR, Millard-Ball A, Hampshire RC, 2020 *Parking search caused congestion: Where's all the fuss? Transportation Research Part C: Emerging Technologies* 120:102781.

Yang S, Qian ZS, 2017 *Turning meter transactions data into occupancy and payment behavioral information for on-street parking. Transportation Research Part C: Emerging Technologies* 78:165–182.